

W 4 D418d 2007
Deo, Shekhar H.
Delta opioid receptor

UNTHSC - FW



M03CIZ

LEWIS LIBRARY
UNT Health Science Center
3500 Camp Bowie Blvd.
Ft. Worth, Texas 76107-2699



Deo, Shekhar H., Delta Opioid Receptor: Parasympathetic Location and Changing Phenotypes in Canine Heart. Doctor of Philosophy (Integrative Physiology), July 23, 112 pp, 4 tables, 24 figures.

Delta opioid receptors (DOR) have long been implicated in the complex mechanism of ischemic preconditioning (IPC). Repeated arterial occlusion of the SA node artery in IPC protocol progressively raised the nodal enkephalin concentrations and improved vagal transmission during a subsequent extended occlusion. This vagotonic effect was reversed by the DOR-1 antagonist, BNTX. The present thesis tested whether the IPC protocol, the prolonged occlusion or a combination of both was required to demonstrate the vagotonic effect. The study also tested whether the evolution of the vagotonic effect during occlusion might be attributed to erosion of competing vagolytic effects. A progressive improvement in vagal transmission was observed during the IPC protocol. The vagotonic effect was not observed during sham occlusions or during occlusions in animals pretreated with a DOR-1 antagonist. Following the IPC protocol, exogenous MEAP reduced vagal transmission under both normal and occluded conditions. The magnitude of the vagolytic effects was however significantly reduced and eroded further over time compared to time matched shams. The loss of the response was not altered by prior DOR-1 blockade. The data confirms that the vagotonic response is mediated by DOR-1. The magnitude of the vagolytic effects was however significantly reduced and eroded further over time compared to time matched shams, however the

failure of DOR-1 blockade to slow that process suggests the PC mediated erosion is independent of receptor activation by DOR-1 agonists.

Although DORs are associated with IPC, their precise location remains unconfirmed. DOR and autonomic markers vesicular acetylcholine transporter (VACHT) and tyrosine hydroxylase (TH) were labeled in tissue sections and synaptosomes from canine atrium and SA node. Synapsin I verified the neural character of labeled structures. Acetylcholine and norepinephrine content indicated both cholinergic and adrenergic synaptosomes are present. VACHT and TH signals indicated more than 80% of synapsin positive synaptosomes were cholinergic and less than 8% were adrenergic. Western blots of synaptosomal extracts confirmed two DOR bands at molecular weights corresponding to reports for DOR monomers and dimmers. The preferential association of DORs with cholinergic nerve terminals supports the hypothesis that post-ganglionic prejunctional DORs regulate local vagal transmission within the heart.

DELTA OPIOID RECEPTOR: PARASYMPATHETIC LOCATION AND
CHANGING PHENOTYPES IN CANINE HEART

Shekhar H. Deo, M.S., M.B.B.S.

APPROVED:

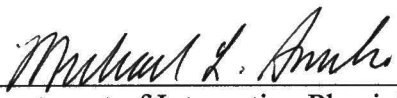

Major Professor: *James L. Caffrey, Ph.D.*

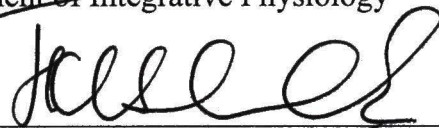

Committee Member: *H. Fred Downey, Ph.D.*


Committee Member: *Michael Smith, Ph.D.*


Committee Member: *Albert Olivencia-Yurvati, D.O.*


University Member: *Michael Forster, Ph.D.*


Chair, Department of Integrative Physiology


Dean, Graduate School of Biomedical Sciences

**DELTA OPIOID RECEPTOR: PARASYMPATHETIC LOCATION AND
CHANGING PHENOTYPES IN CANINE HEART**

DISSERTATION

**Presented to the Graduate Council of the
Graduate School of Biomedical Sciences
University of North Texas
Health Science Center at Fort Worth**

In Partial Fulfillment of the Requirements

For the Degree of

DOCTOR OF PHILOSOPHY

By

Shekhar H. Deo, M.S., M.B.B.S.

Fort Worth, Texas

July 2007

ACKNOWLEDGEMENTS

This project was supported by the Texas ARP grant at the University of North Texas Health Science Center.

My endeavor was not possible without the generous support, guidance and expertise of my mentor, Dr. James L. Caffrey. I express my sincere gratitude for his extreme patience for giving me the determination to complete what at times appeared impossible to me. I would like to thank the members of my committee, Dr. H. Fred Downey, Dr. Michael Smith, Dr. Albert O-Yurvati and Dr. Michael Forster for their guidance and support throughout my studies. I would also like to thank my laboratory members Matthew Barlow, Leticia Gonzalez, Darice Yoshishige and Dr. Arti Sharma for their valuable inputs to and help with these studies. I express my thanks and appreciate the laboratories of Dr. Margaret Garner of the Department of Cell Biology and Genetics, Dr. Jerry Simecka and Dr. Harlan Jones of the Department of Molecular Biology and Immunology, and Dr. Thomas Yorio for their kind guidance in the respective fields of expertise and allowed me to use their cutting-edge tools and equipments for the completion of this study. I am very much grateful to my friend and colleague, Vidhya Rao of Dr. Yorio's lab who performed the western blots. Members and staff of the Graduate School of Biomedical Sciences and Department of Integrative Physiology were very much a part of my experiences during my graduate career. I am very fortunate to have Mrs. Pramila H. Deo and Dr. Hari T. Deo as my parents and I express my sincere gratitude to them.

PUBLICATIONS

- **Deo SH, Barlow MA, Gonzalez L, Yoshishige D, and Caffrey JL.** Cholinergic Location of Delta Opioid Receptors in Canine Atria and SA Nod. *Am J Physiol Heart Circ Physiol*, 2007; H-00141.
- **Deo SH, Barlow MA, Gonzalez L, Johnson S, Yoshishige D, and Caffrey JL.** Preconditioning, Delta-Opioid Receptor (DOR) Plasticity and Vagal Transmission within the Sinoatrial Node. (Submitted)
- **Deo S, Barlow MA, Johnson S, Daniel N, and Caffrey JL.** Repeated δ_1 -opioid receptor stimulation down regulates δ_2 -opioid receptor responses **Deo SH, Johnson-Davis S, Barlow MA, Yoshishige D and Caffrey JL.** Repeated delta1-opioid receptor stimulation reduces delta2-opioid receptor responses in the SA node. *Am.J.Physiol.Heart Circ.Physiol.* 291: 5: H2246-54, 2006.
- **Davis S, Deo SH, Barlow M, Yoshishige D, Farias M and Caffrey JL.** The monosialosyl ganglioside GM-1 reduces the vagolytic efficacy of delta-2-opioid receptor stimulation. *Am.J.Physiol.Heart Circ.Physiol.* 291: 5: H2318-26, 2006.
- **Vinogradoca TM, Lyashkov AE, Zhu W, Ruknudin AM, Sirenko S, Yang D, Deo S, Barlow M, Johnson S, Caffrey JL, Zhou Y, Xiao P, Cheng H, Stern MD, Maltsev VA, and Lakatta EG.** High basal protein kinase A-dependent phosphorylation drives rhythmic internal Ca^{2+} store oscillations and spontaneous beating of cardiac pacemaker cells. *Circ Res* 98: 505-514, 2006.

- **Barlow MA, Deo S, Johnson S, and Caffrey JL.** Vagotonic effects of enkephalin are not mediated by sympatholytic mechanisms. *Exp Bio Med* 231: 387-402, 2006.
- **Olivencia-Yurvati AH, Mallet RT, Ortolano GA, Paul G, Barlow MA, Deo S, Daniel N, Johnson S, and Caffrey JL.** Leukocyte filtration for off-pump coronary artery bypass. *Filtration 2*: 57-69, 2005.
- **Stanfill A, Jackson KE, Farias M, Barlow M, Deo S, Johnson S, and Caffrey JL.** Leucine-Enkephalin interrupts sympathetically mediated tachycardia prejunctionally in the canine sinoatrial node. *Exp Bio Med* 228: 898-906, 2003.

ABSTRACTS

- **Deo S, Barlow MA, Yoshishige D, and Caffrey JL.** 4-tyrosyl-enkephalins are inactive in heart compared to their vagolytic 4-phenylalanyl-parents, met- and leu-enkephalin. *FASEB J* 20: A1201, 2006.
- **Barlow MA, Deo S, and Caffrey JL.** Enkephalin modulation of hind limb blood conduction. *14th Annual RAD UNTHSC*: 42, 2006.
- **Gonzalez L, Barlow MA, Deo S, Yoshishige D, Jones H and Caffrey JL.** Proenkephalin derived peptides in canine neutrophils. *14th Annual RAD UNTHSC*: 39, 2006.
- **Barlow MA, Deo S, Johnson S, and Caffrey JL.** Vagotonic effects of enkephalin are not mediated by sympatholytic mechanisms. *FASEB J* 19: A1303, 2005.
- **Barlow MA, Daniel N, Deo S, Johnson S, Yoshishige D, and Caffrey JL.** Vagotonic effects of enkephalin are not mediated by sympatholytic mechanisms. (12th annual Research Appreciation Day) University of North Texas Health Science Center, 2004.
- **Caffrey JL, Deo S, Barlow MA, Johnson S, and Farias M.** Opioid-Ganglioside interactions during vagal bradycardia. *FASEB J* 18: A1074, 2004.

- **Deo S, Barlow MA, Johnson S, Daniel N, and Caffrey JL.** Repeated arterial occlusions improve vagal transmission in the sinoatrial node without eliminating the vagolytic response to opioids. *FASEB J* 19: A708, 2005.
- **Johnson-Davis S, Deo S, Barlow MA, Yoshishige D, and Caffrey JL.** GM-1, Deltorphin, and δ -2 receptor plasticity in the SA Node. *FASEB J* 19: A1322, 2005.
- **Stanfill A, Jackson K, Farias M, Barlow M, Deo S, Johnson S, and Caffrey JL.** Kappa-opioid receptors in the cardiac pacemaker decrease sympathetic tachycardia. (11th annual Research Appreciation Day) University of North Texas Health Science Center, 2003.

TABLE OF CONTENTS

ACKNOWLEDGEMENTS.....	vi
-----------------------	----

LIST OF ILLUSTRATIONS.....	xiii
----------------------------	------

I. CHAPTER I

Introduction.....	1
Specific Aims.....	14
References.....	16

II. CHAPTER II

PRECONDITIONING, DELTA-OPIOID RECEPTOR (DOR) PLASTICITY AND VAGAL TRANSMISSION WITHIN THE SINOATRIAL NODE.

Abstract.....	22
Introduction.....	23
Methods.....	28
Results.....	34
Discussion.....	40
References.....	46
Legends.....	52
Figures.....	54

III. CHAPTER III

CHOLINERGIC LOCATION OF DELTA OPIOID RECEPTORS IN CANINE ATRIA AND SA NODE.

Abstract.....	64
Introduction.....	66
Methods.....	69
Results.....	76
Discussion.....	85
References.....	91
Legends.....	97
Figures.....	101

IV. CONCLUSION.....	111
V. SUGGESTIONS FOR FUTURE RESEARCH.....	112

LIST OF ILLUSTRATIONS

I.	CHAPTER I		
	FIGURE 1.	Proposed bimodal mechanism.....	10
II.	CHAPTER II		
	TABLE 1.	Resting Cardiovascular Indices.....	54
	FIGURE 1	IPC improves vagotonic responses.....	55
	FIGURE 2a	Time Controls: Vehicle and Duration.....	56
	FIGURE 2b.	Time Controls: vehicle, duration, and OC5.....	57
	FIGURE 3.	DOR-1 blockade prevented IPC mediated improvement in vagotonic response.....	58
	FIGURE 4.	Influence of IPC on DOR-2 responses.....	59
	FIGURE 5a.	Influence of vehicle and duration on DOR-2 responses.....	60
	FIGURE 5b.	Influence of vehicle, duration, and OC5 on DOR-2 responses.....	61
	FIGURE 6.	Influence of IPC+DOR-1 blockade on DOR-2 responses.....	62
III.	CHAPTER III		
	TABLE 1.	Immunocytochemical Labelling of Synaptosomes.....	101
	TABLE 2.	Immunocytochemical Labelling of Tissue Sections.....	102
	TABLE 3	Catecholamine measurements in synaptosomes.....	103
	FIGURE 1a.	Nodal Artery: DOR.....	104
	FIGURE 1b	Nodal Artery: Synapsin.....	104
	FIGURE 1c	Nodal Artery: Merge (DOR and Synapsin).....	104
	FIGURE 1d	Nodal Artery: Merge (Control RIgG and GIgG).....	105
	FIGURE 2a.	Nodal Artery and Tissue: DOR.....	106
	FIGURE 2b.	Nodal Artery and Tissue: VACHT.....	106
	FIGURE 2c.	Nodal Artery and Tissue: Merge (DOR and VACHT).....	106
	FIGURE 3a.	Nodal Artery: Merge (DOR and VACHT) 40X under Confocal Microscope.....	107
	FIGURE 3b.	Right Atrial Muscle: Merge (DOR and VACHT) 40X under Confocal Microscope.....	107
	FIGURE 4a.	Nodal Artery: DOR.....	108
	FIGURE 4b.	Nodal Artery: TH.....	108
	FIGURE 4c.	Nodal Artery: Merge (DOR and TH).....	108

FIGURE 5.	Tissue: Co-localization Quantification.....	109
FIGURE 6.	Synaptosome: Co-localization Quantification.....	109
FIGURE 7a	Synaptosomes: Western Blot	110
FIGURE 7b.	Densitometric Analysis of Synaptosomal Western Blot.....	110

CHAPTER I

INTRODUCTION

Historical Perspective

Opium, one of the oldest known medicinal was often used by man for its mind altering properties. The ancient Greeks and Romans were fully aware of the euphoric and analgesic effects of opium and therefore administered the drug for a variety of maladies and for recreational purposes. It is extracted from opium poppy, *Papaver somniferum*. Opioids are peptide sequences possessing pharmacological and biochemical properties similar to that of opium. In 1805, German chemist Friedrich Serturmer isolated the active principle in opium and named it morphine, after Morpheus, the Greek God of dreams. In the nineteenth century, opioid abuse became a major problem in America. Today, a variety of opiates are used legally as analgesics, cough suppressants and as antidiarrheal agents. Endogenous opioids are opioid peptide sequences synthesized by the body itself that have similar properties to that of opium.

Endogenous Opioids in Heart

Endogenous cardiac opioids are potent modulators of cardiovascular function with significant physiological and pathological influences. The opioid peptides discovered thus far include the dynorphins, enkephalins, endorphins and endomorphins. The peptides are synthesized as precursor molecules and the constituent opioid peptide(s) are released by selective hydrolysis. Proenkephalin for instance includes four copies of methionine-enkephalin (ME), one copy of methionine-enkephalin-arginine-phenylalanine (MEAP), one copy of leucine-enkephalin (LE) and one copy of methionine-enkephalin-arginine-glycine-leucine (MEAGL). Proenkephalin mRNA was found more abundant in heart than in other tissues (10, 17, 30, 32). Surprisingly, MEAP was more concentrated in heart than ME despite the higher copy number for ME in the precursor (32). MEAP, ME and LE alter the vagally mediated decline in heart rate when introduced directly in the SA node by microdialysis (5, 12, 13). Opioids can improve or impair vagal transmission by binding to specific opioid receptors. The probable location of these opioid receptors is on the prejunctional, postganglionic vagal nerve terminals within the SA node (3).

Endogenous Opioid Receptors

Opioid receptors belong to the family of G-protein coupled receptors (GPCR). Upon binding, opioids activate various downstream pathways to regulate neurotransmitter release (9, 18, 20). There are three classes of opioid receptors designated

as mu (μ), kappa (κ) and delta (δ) receptors. The native enkephalins bind with high affinity to delta opioid receptors (DORs) and behave as potent DOR-agonists. Pharmacological studies indicated that there are two distinct DOR phenotypes despite biochemical analysis in support of a single protein transcript (1, 5, 18, 20, 30). Farias et al demonstrated that the DORs modulated vagal transmission bimodally in canine SA node. Lower concentrations of enkephalin enhanced vagal transmission (vagotonic) and higher concentrations reduced the vagal transmission (vagolytic) (5). The two opposing effects were blocked by subtype specific antagonists implicating DOR subtypes in opposing responses.

Repeated arterial occlusion increases enkephalin in SA node and improves vagal function.

Endogenous opioid peptides function as neuromodulators in a wide variety of biological systems. However, their function in the cardiovascular system is not well understood. The opioid peptides are widely distributed in the peripheral autonomic nervous system where they most likely regulate neurotransmitter release. MEAP, which is derived from the C-terminal sequence of the proenkephalin is one of the most abundant opiate peptides in the myocardium. When administered into the SA node, MEAP immediately and reversibly blocked vagal control of heart rate. Jackson et al demonstrated that repeated arterial occlusions in the preconditioning protocol raised the nodal MEAP content and coincided with the improvement in the vagal function. This improvement was mediated by DOR-1 (13). MEAP concentration was low prior to

occlusion of the SA node artery but rose dramatically in the dialysate during each subsequent occlusion. The increase in MEAP recovered during arterial occlusion suggested a progressive increase peptide release into the nodal interstitium. An increased capacity for enkephalin release during repeated occlusions might be consistent with the putative role of opioids in ischemic preconditioning. When the vagus nerve was stimulated during the subsequent sustained occlusion, its function was significantly improved. Also, the enhancement in vagal transmission following the preconditioning protocol was blocked by a selective DOR-1 antagonist, suggesting again the DOR-1 participated in preconditioning (21). DOR-1 stimulation improved the vagal transmission and may contribute to cardioprotection by reducing local myocardial oxygen demand and thus ischemic damage following coronary occlusion. The finding that the increase in the local endogenous MEAP improved vagal function was contrary to the expectation since exogenous administration of MEAP delivered by nodal dialysis suppressed vagal function. These contradictory observations suggested that either the increase in endogenous peptide was coincident and unrelated to the vagal improvement or that the polarity of the response shifted dramatically during low flow conditions.

Bimodal effects of DOR stimulation on vagal function in SA node.

Further, our laboratory demonstrated that cardiac enkephalins regulate the vagal function in the bimodal manner (5). Exogenous administration of ultra-low doses of MEAP (500 fmol/min infusion rate) into the SA node by the microdialysis improves the vagal function (vagotonic response). Specific DOR-1 antagonist, BNTX, blocks this improvement. However, administration of high doses (5 nmol/min infusion rate) of MEAP reduces the vagal function (vagolytic response). This effect was blocked by naltriben, a specific DOR-2 antagonist. Thus, enkephalins act on the two phenotypes of DOR in a concentration dependent manner.

Crain et al demonstrated both excitatory and inhibitory pathways in dorsal root ganglion (DRG) cells and suggested that opiate receptor polarity might shift between these modes. They proposed that excitatory mode activates the adenylyl cyclase-cAMP-PKA pathway, as illustrated in Figure 1, by coupling through the G-protein, G_{sa} . The consequent protein kinase A (PKA) activation then led to the prolongation of the action potential duration of the DRG cells followed by a subsequent decrease in the neurotransmitter release (4, 28). The present study was based on related observations made in the SA node. The working hypothesis proposes that ultra low concentrations of enkephalins stimulate the G_{sa} -coupled δ_1 -receptors on vagal nerve terminal and increase acetylcholine release in the SA node. On the other hand, higher concentrations of enkephalin stimulate $G_{i/o}$ -coupled δ_2 -receptors that decrease the acetylcholine release (5).

Crain and Shen proposed that the quality and sensitivity of the response was governed by the ganglioside content of the neural cell membrane surrounding the opiate receptor. Membranes rich in the monosialosyl-ganglioside, GM1 favored excitatory opioid responses at very low doses. The excitatory response was further proposed to activate a positive feedback loop that increased its own excitatory activity by stimulating the synthesis of more GM1. Ultra-low opioid concentrations stimulate δ_1 -opioid receptors coupled through G_s to activate adenylyl cyclase. The hypothesis suggested that the resulting increase in the cyclic-AMP dependent protein kinase, phosphorylated the glycosyl transferase enzyme, and increased the synthesis of GM1. This increase in GM1 theoretically improved the efficiency of excitatory opioid receptor coupling and counteracted the inhibitory opioid receptor effects. In the absence of GM1 the same opioids reduced adenylyl cyclase activity through G_i/G_o -coupling (3, 4). Thus, they suggested that the excitatory stimulation and the resulting changes in the environment around the receptor modified the response in isolated systems (28, 31).

The existence of a single DOR transcript and two functional opposing responses, suggested that inter-conversion between the two subtype populations might be physiologically important. The subtype inter-conversion during preconditioning might shift the balance of responses in favor of a cardioprotective DOR-1. Preliminary observations indicated a reduction in the intensity of DOR-2-mediated vagolytic response following the exposure of the SA node to extended DOR-1 stimulation.

Sustained DOR-1 stimulation down-regulates DOR-2 responses.

Preliminary studies have demonstrated that extended exposure to DOR-1 stimulation down regulates DOR-2 responses in the SA node. The hypothesis was formulated from previous observations that dose responses to DOR-1-agonists were followed by a dramatic reduction in the subsequent DOR-2-mediated vagolytic responses. Prior nodal exposure to the DOR-1-agonist, TAN 67 eroded the vagolytic effect of the DOR-2-agonist, deltorphin II. The heterologous participation by DOR-1 was verified when the selective DOR-1-antagonist, BNTX prevented the loss of the DOR-2-response. These results led to the suggestion that DOR-1 stimulation reduced subsequent DOR-2 mediated vagolytic responses.

GM1 treatment enhances the DOR-1-response and reduces the DOR-2 response.

The initial observations made in the heart are consistent with those made in sensory neurons that opioids were excitatory in some circumstances and inhibitory in others (3). Since only one transcript has been isolated for the DOR, we have suggested that the DOR coupling in the SA node is fluid and the receptor phenotypes might be inter-convertible. Pretreatment with a sub-threshold dose of MEAP had no effect on vagal transmission. Higher dose MEAP reduced the decline in heart rate by two thirds. GM1 had no demonstrable effect on the control response. However after treatment with

GM1, the vagolytic effect of high MEAP was reduced and a clear vagotonic effect of low MEAP emerged. These data support the hypothesis that GM1 improved the DOR-1-mediated vagotonic effect of MEAP at the expense of a decline in its DOR-2-mediated vagolytic effect.

Like high dose of MEAP, deltorphin (selective DOR-2 agonist) produced a significant vagolytic response when first introduced in to the nodal interstitium. The GM1 treatment had no measurable effect on the vagal responses during the 60-minute treatment period, but the subsequent vagolytic responses were progressively reduced in magnitude. These data suggest that GM1 suppresses the DOR-2 response. However, BNTX was ineffective in altering the subsequent erosion of the DOR 2-response. The progressive attrition of the response was very similar to that observed in the study without BNTX suggesting that as an intermediate, GM1 bypasses the requirement for DOR-1 stimulation.

Presynaptic Location of Delta Opioid Receptors (DOR) on the Parasympathetic Nerve Terminals

Although endogenous enkephalins function as neuromodulators, their actions to inhibit or facilitate the release of neurotransmitters depend on the local concentrations of these peptides at DORs. The observation that enkephalins inhibit vagal transmission in canine SA node is well supported by prior studies. However, the exact location of such a

receptor in the node is still undetermined. Systemic administration of MEAP did not alter the negative chronotropic effect of the direct acting muscarinic agonist; methacholine (9). The inability to alter the response to methacholine suggested that MEAP exerted its effect at a site in the efferent vagal tract that is proximal to the nodal post-synaptic muscarinic receptors. This narrows the location of these opiate receptors to sites within the intracardiac parasympathetic ganglia or at prejunctional sites (e.g. vagal nerve terminals) within the sinoatrial node. When MEAP was infused directly into the sinoatrial node via the microdialysis probe, it reduced the vagal transmission significantly (10). Such reduction in vagal transmission was observed only when the vagus nerve was stimulated. There was no effect of MEAP on the un-stimulated vagus nerve suggesting the role of enkephalins in inhibiting acetylcholine release from the parasympathetic nerve terminals. Simultaneous local nodal blockade of these receptors with the opiate antagonist, diprenorphine, eliminated the effect of MEAP demonstrating the participation by opiate receptors. These data lead us to suggest that DOR responsible for the inhibition of vagal transmission are located within the sinoatrial node on the presynaptic parasympathetic nerve terminals. As mentioned earlier, DORs belong to the super family of G-protein coupled receptors with seven transmembrane spanning structural motifs (6). The identification of such receptor motif has now made possible to determine the exact anatomical location of DOR by immunocytochemistry with antibodies directed against the predicted sequence of amino acids in the receptors.

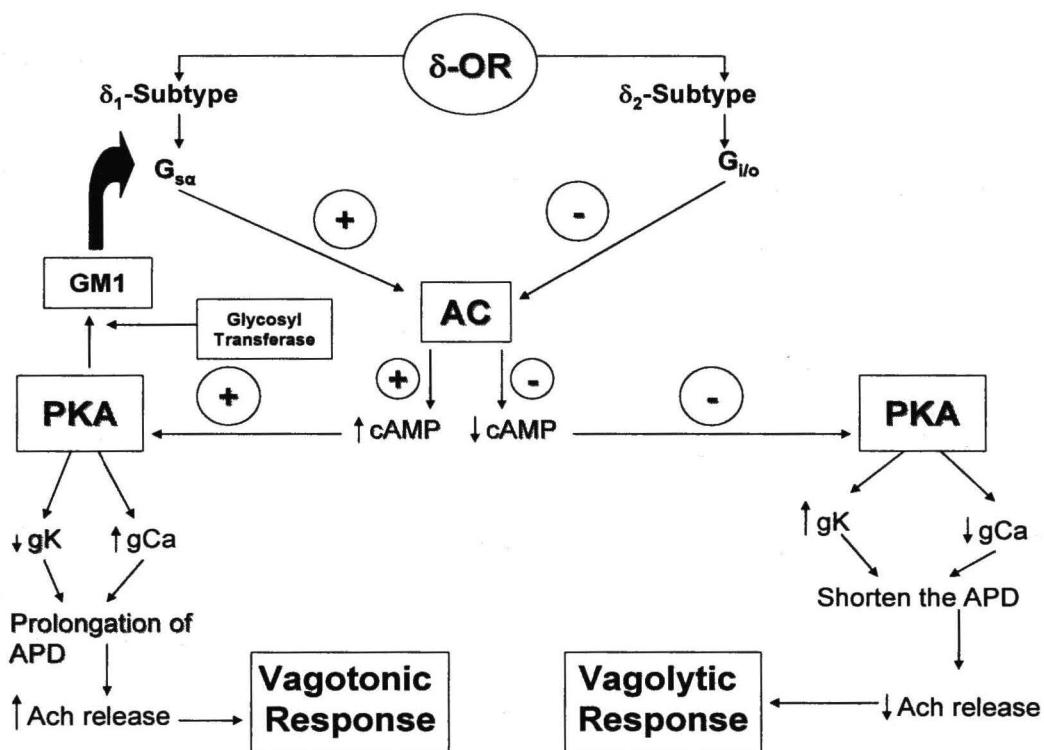


Figure 1: The figure illustrates how the opposing DOR interactions might translate into changes in neurotransmitter release. The DOR-1-phenotype couples with the G_{sa} protein to activate the adenylyl cyclase enzyme (AC) and increase cyclic adenosine monophosphate (cAMP) concentration. CAMP in turn activates protein kinase A (PKA). PKA phosphorylates the voltage gated K^+ and Ca^{++} channels to increase Ca^{++} and K^+ conductance (g_K and g_{Ca}). PKA also activates glycosyl transferase to increase the synthesis of neural membrane ganglioside (GM1). GM1 enhances DOR-1/ G_{sa} -coupling to complete a positive-feedback loop to prolong the action potential duration (APD) of the vagal nerve membrane. Thus acetylcholine (Ach) secretion increases and vagal transmission improves. Reciprocal effects occur at the DOR-2-phenotype as it couples with the $G_{i/o}$ protein to cause inhibition of the AC. This leads to further reduction in all

the components of the pathway shown in the figure to reduce the vagal transmission. GM1 does not directly alter the coupling of the DOR-2/ $G_{i/o}$ coupling.

Summary

1. The preconditioning like protocol raises the nodal enkephalin content.
2. Enkephalins exert bimodal effects on vagal function at the SA node.
3. Extended DOR-1 stimulation reduces the vagolytic response to DOR-2 stimulation.
4. Blocking the DOR-1 agonist with BNTX prevents the attrition of vagolytic response.
5. GM1 simultaneously enhanced the DOR-1 mediated vagotonic response to MEAP and reduced the vagolytic DOR-2 response.

Significance

Myocardial infarction (MI) is the leading cause of morbidity and mortality in the United States. Approximately 1.3 million cases of nonfatal MI are reported each year, for an annual incidence of approximately 600 per 100,000 people. Approximately 500,000-700,000 deaths are caused by ischemic heart disease annually in the United States (2). Myocardial infarction occurs when myocardial ischemia exceeds a critical threshold and overwhelms the cellular repair mechanisms that are designed to maintain normal operating function. Myocardial ischemia may occur as a result of increased metabolic demand and/or decreased coronary delivery of oxygen to the myocardium. Opioids are implicated in ischemia preconditioning and cardioprotection. Repeated occlusion of the

SA node artery in a preconditioning-like protocol raised enkephalins locally and improved vagal transmission (13). The improvement in vagal function in the ischemic region might thus preserve the ischemic myocardium by reducing work and oxygen demand locally (16). DOR-1 and improved vagal transmission are associated with the cardioprotection (23, 26). Also, the DOR-1-mediated reduction in DOR-2 responses may reinforce the cardioprotective efficacy of DOR-1 agonists (25). Finally, the gradual increase in the DOR-2-response in untreated controls may reflect a mechanism by which DOR-2 contributes to the gradual closure of the initial window of cardioprotection that follows ischemic preconditioning. Thus far the locations of DORs have remained obscure. The localization of such receptors will help direct therapeutic strategies to induce cardioprotection pharmacologically.

HYPOTHESES

Sustained DOR-1 stimulation due to ischemic preconditioning down-regulates the vagolytic response of the DOR-2 in the canine sinoatrial node. The following study is designed to determine whether preconditioning or simply the prolonged ischemia is responsible for the observed vagotonic effect. The study will also test whether MEAP is vagotonic during ischemia because competing vagolytic effects are abolished.

The precise location of delta opioid receptors is on the postganglionic presynaptic parasympathetic nerve terminals in the canine SA node.

Specific Aim # 1: To test whether the functional improvement of DOR-1 during ischemic preconditioning reduces subsequent DOR-2 responses.

Hypothesis 1A: To test whether preconditioning is required for the improved vagal function during arterial ischemia. The heart will be exposed from the right side and a microdialysis probe will be introduced into the SA node. The nodal artery will be occluded and reperfused in 5 twenty min cycles. The right vagus nerve will be stimulated intermittently to evaluate when the vagotonic effect appears.

Hypothesis 1B: To test whether repeated SA node arterial occlusions gradually improve the vagal function mediated by DOR-1 by abolishing the vagolytic responses mediated by DOR-2. Following the preconditioning-like protocol, MEAP will be introduced into the SA node via microdialysis (11) during occlusion and reperfusion. Vagal stimulation will be performed in the presence of MEAP to assess the changes in the DOR-2 receptor response. Sham dogs will undergo similar surgical procedures; however no preconditioning occlusions will be conducted on the nodal artery.

Specific Aim#2: To test whether blocking the opposing DOR-1 mediated vagotonic response with BNTX prevents the attrition of vagolytic response. The preconditioning-like protocol will be performed and the DOR-1-specific antagonist, BNTX will be delivered into the SA node via the microdialysis to block the effects of preconditioning.

Specific Aim # 3: To determine the location of DORs in heart. DORs will be assessed by immunohistochemistry in the nodal tissue and by immunocytochemistry in isolated synaptosomes.

REFERENCES

1. **Allouche S, Hasbi A, Frey V, Sola B, Jauzak P, and Polastron J.** Pharmacological δ_1 - and δ_2 -opioid receptor subtypes in the human neuroblastoma cell line SK-N-BE: no evidence for distinct molecular entities. *Biochem Pharmacol* 59: 915-925, 2000.
2. **Brown AL, Mann NC, and Daya M.** Demographic, belief, and situational factors influencing the decision to utilize emergency medical services among chest pain patients. Rapid Early Action for Coronary Treatment (REACT) study. *Circulation* 102(2): 173-8, 2000.
3. **Caffrey JL, Mateo Z, Napier LD, Gaugl JF, and Barron BA.** Intrinsic cardiac enkephalins inhibit vagal bradycardia in the dog. *Am J Physiol Heart Circ Physiol* 268: H848-855, 1995.
4. **Crain SM and Shen KF.** After chronic opioid exposure sensory neurons become supersensitive to the excitatory effects of opioid agonists and antagonists as occurs after acute elevation of GM1 ganglioside. *Brain Res* 575 (1): 13-24, 1992.
5. **Farias M, Jackson KE, Yoshishige D, and Caffrey JL.** Bimodal δ -opioid receptors regulate vagal bradycardia in canine sinoatrial node. *Am J Physiol Heart Circ Physiol* 285 (3): H1332-H1339, 2003.
6. **Farias M, Jackson KE, Stanfill AS, and Caffrey JL.** Local opiate receptors in the sinoatrial node moderate vagal bradycardia. *Auton Neurosci* 87 (1): 9-15, 2001.

7. **Farias M, Jackson KE, Yoshishige D, and Caffrey JL.** Cardiac enkephalins interrupt vagal bradycardia via δ_2 -opioid receptors in sinoatrial node. *Am J Physiol Heart Circ Physiol* 284 (5): H1693-H1701, 2003.
8. **Farias M, Jackson KE, Johnson M, and Caffrey JL.** Cardiac enkephalins attenuate vagal bradycardia: interactions with NOS-1-cGMP systems in canine sinoatrial node. *Am J Physiol Heart Circ Physiol* 285 (5): H2001-12, 2003.
9. **Grady EF, Bohm SK, and Bunnett NW.** Turning off the signal: mechanisms that attenuate signaling by G protein-coupled receptors. *Am J Physiol* 273: 586-601, 1997.
10. **Howells RD, Kilpatrick DL, Bailey LC, Noe M, and Udenfriend S.** Proenkephalin mRNA in rat heart. *Proc Natl Acad Sci USA* 83 (6): 1960-1963, 1986.
11. **Imamura M, Seyedi N, Lander HM, and Levi R.** Functional identification of histamine H3-receptors in human heart. *Circ Res* 77: 206-210, 1995.
12. **Jackson KE, Farias M, and Caffrey JL.** Cardiac microdialysis a powerful tool. *Cardiovasc Res* 46 (3): 367-369, 2000.
13. **Jackson KE, Farias M, Stanfill AS, and Caffrey JL.** Transient arterial occlusion raises enkephalin in the canine sinoatrial node and improves vagal bradycardia. *Auton Neurosci* 94 (1-2): 84-92, 2001.
14. **Jackson KE, Farias M, Stanfill AS, and Caffrey JL.** Delta opioid receptors inhibit vagal bradycardia in the sinoatrial node. *J Cardiovasc Pharmacol Ther* 6 (4): 385-393, 2001.

15. **Kawate T, Sakamoto H, Yang C, Li Y, Shimada O, Atsumi S.** Immunohistochemical study of delta and mu opioid receptors on synaptic glomeruli with substance P-positive central terminals in chicken dorsal horn. *Neurosci Res* 53(3): 279-87, 2005.
16. **Kleiger RE, Miller JP, Bigger JT Jr, and Moss AJ.** Decreased heart rate variability and its association with increased mortality after acute myocardial infarction. *Am J Cardiol* 59 (4): 256-262, 1987.
17. **Lang RE, Hermann K, Dietz R, Gaida W, Ganten D, Kraft K, and Unger T.** Evidence for the presence of enkephalins in the heart. *Life Sci* 32 (4): 399-406, 1983.
18. **Loh HH, and Smith AP.** Molecular characterization of opioid receptors. *Annu Rev Pharmacol Toxicol* 30: 123-147, 1990.
19. **LoPachin RM, Schwarcz AI, Gaughan CL, Mansukhani S, Das S.** In vivo and in vitro effects of acrylamide on synaptosomal neurotransmitter uptake and release. *Neurotoxicology* 25(3): 349-63, 2004.
20. **Martin WR.** Pharmacology of opioids. *Pharmacol Rev* 35: 283-323, 1984.
21. **Portoghese PS, Sultana M, Nagese H, and Takemori AE.** A highly selective δ_1 -receptor antagonist: 7-benzylidenaltrexone. *Eur J Pharmacol* 218: 195-196, 1992.
22. **Rousseau SJ, Jones IW, Pullar IA, Wonnacott S.** Presynaptic $\alpha 7$ and non- $\alpha 7$ nicotinic acetylcholine receptors modulate [3 H]d-aspartate release from rat frontal cortex in vitro. *Neuropharmacology* 49(1): 59-72, 2005.

23. **Schultz JE, Rose E, Yao Z, and Gross GJ.** Evidence for involvement of opioid receptors in ischemic preconditioning in rat hearts. *Am J Physiol Heart Circ Physiol* 268: H2157–H2161, 1995.
24. **Schultz JE, Hsu AK, and Gross GJ.** Ischemic preconditioning is mediated by a peripheral opioid receptor mechanism in the intact rat heart. *J Mol Cell Cardiol* 29 (5): 1355-1362, 1997.
25. **Schultz JE, Hsu AK, Nagese H, and Gross GJ.** TAN-67 a δ_1 -opioid receptor agonist, reduces infarct size via activation of $G_{i/o}$ proteins and K_{ATP} channels. *Am J Physiol Heart Circ Physiol* 274: H909-H914, 1998.
26. **Schultz JE, Hsu AK, and Gross GJ.** Ischemic preconditioning in the intact rat heart is mediated by δ_1 - but not μ - or κ -opioid receptors. *Circulation* 97 (13): 1282-1289, 1998.
27. **Seyedi N, Koyama M, Mackins CJ, and Levi R.** Ischemia promotes rennin activation and angiotensin formation in sympathetic nerve terminals isolated from the human heart: Contribution to carrier-mediated norepinephrine release. *J Pharmacol Exp Ther* 302: 539-544, 2002.
28. **Shen KF, and Crain SM.** Cholera toxin-B subunit blocks excitatory effects of opioids on sensory neuron action potentials indicating that GM1 ganglioside may regulate Gs-linked opioid receptor functions. *Brain Res* 531: 1-7, 1990.
29. **Sofuoglu M, Portoghese PS, and Takemori AE.** Differential antagonism of δ -opioid agonists by naltrindole and its benzofuran analog (NTB) in mice: evidence for δ -opioid receptor subtypes. *J Pharmacol Exp Ther* 257 (2): 676-680, 1991.

30. **Springhorn JP and Claycomb WC.** Translation of heart preproenkephalin mRNA and secretion of enkephalin peptides from cultured cardiac myocytes. *Am J Physiol Heart Circ Physiol* 263: H1560-H1566, 1992.
31. **Wu G, Lu ZH, and Ledeen RW.** Interaction of δ -opioid receptors with GM-1 ganglioside: Conversion of inhibitory to excitatory mode. *Mol Brain Res* 44: 341-346, 1997.
32. **Younes A, Pepe S, Barron BA, Surgeon HA, Lakatta EG, and Caffrey JL.** Cardiac synthesis, processing, and coronary release of enkephalin-related peptides. *Am J Physiol Heart Circ Physiol* 279 (4): H1989-H1998, 2000.
33. **Zaki PA, Bilsky EJ, Vanderah TW, Lai J, Evans CJ, and Porreca F.** Opioid receptor types and subtypes: the δ -receptor as a model. *Annu Rev Pharmacol Toxicol* 36: 379-401, 1996.
34. **Zsembery A, Boyce AT, Liang L, Peti-Peterdi J, Bell PD, Schwiebert EM.** Sustained calcium entry through P2X nucleotide receptor channels in human airway epithelial cells. *J Biol Chem* 278(15): 13398-408, 2003.

CHAPTER II

Preconditioning, Delta-Opioid Receptor (DOR) Plasticity and Vagal Transmission within the Sinoatrial Node.

Shekhar H. Deo, Matthew A. Barlow, Leticia Gonzalez, Darice Yoshishige, and James L. Caffrey

University of North Texas Health Science Center

Department of Integrative Physiology

3500 Camp Bowie Boulevard

Fort Worth, TX 76107

Corresponding author: James L. Caffrey

University of North Texas Health Science Center

Department of Integrative Physiology

3500 Camp Bowie Boulevard

Fort Worth, TX 76107

Tel. No. 817-735-2085

jcaffrey@hsc.unt.edu

Keywords: DOR Phenotypes, Opioids, Vagal function

Running Title: DOR and Vagal Transmission

ABSTRACT

Brief interruptions in coronary blood flow precondition the heart and reduce the damage that typically accompanies myocardial infarction. Delta opioid receptors (DORs) are involved. Repeated occlusion of the sinoatrial (SA) node artery in an ischemic preconditioning (IPC) protocol progressively raised the nodal methionine-enkephalin-arginine-phenylalanine (MEAP) and improved vagal transmission during subsequent occlusions. The DOR-1 antagonist, BNTX reversed the vagotonic effect. Higher doses of enkephalin interrupted vagal transmission through a DOR-2 mechanism. The current study tested whether the PC protocol, the prolonged occlusion or a combination of both was required for the vagotonic effect. The study also tested whether evolving vagotonic effects included the withdrawal of competing DOR-2 vagolytic influences. Vagal transmission progressively improved during successive occlusions of the SA node artery. The vagotonic effect was absent in shams and after DOR-1 blockade. After completing the PC protocol, vagolytic doses of MEAP reduced vagal transmission under both normal and occluded conditions. The magnitude of the DOR-2 vagolytic effect was small compared to controls and repeated MEAP rapidly eroded the vagolytic response further. Prior DOR-1 blockade accelerated the near complete loss of the DOR-2 vagolytic response. In conclusion, the DOR-1 vagotonic response evolved from PC signals earlier in the protocol. PC mediated erosion of competing DOR-2 vagolytic responses may contribute to unmasking vagotonic responses. The data support the hypothesis that PC

and DOR-2 stimulation promote DOR trafficking, and down regulation of the vagolytic DOR-2 phenotype in favor of the vagotonic DOR-1 phenotype. DOR-1 blockade may accelerate the process by sequestering newly emerging receptors.

INTRODUCTION

Although prevention of heart disease is always a primary goal, coronary occlusions are common and the salvage of injured myocardium afterward has been an important research focus for decades. The prognosis for survival is greater in patients (21) and experimental animals (1) that demonstrate active vagal control of heart rate. Although a number of different autocooids have been implicated as mediators of cardioprotection much of the research has focused on adenosine (13, 25) and opioids (33). Both of these mediators share second messenger systems with another potential mediator, acetylcholine (37). Although multiple mediators are likely to participate, opioids have been widely implicated in ischemic preconditioning (IPC) and in virtually every form of cardioprotection including the more recently described variants of remote conditioning and post-conditioning (15, 28). Thus, robust parasympathetic systems and selective opioid receptor stimulation are commonly associated with improved cardiovascular outcomes following coronary occlusion (38, 39).

The role of opioids in ischemic preconditioning is largely based on the pharmacological studies that demonstrated that opioid antagonists abrogate and added opioids mimic the beneficial effects of ischemic preconditioning (15, 22, 26). The actual contributions of endogenous opioids are more complex and much less well understood (38, 39). Changes in endogenous opioids are however consistent with the

cardioprotective thesis in that coronary occlusion increases available endogenous opioids in the myocardial interstitium (19).

Endogenous opioid peptides function as neuromodulators in a wide variety of biological systems and commonly exert an acute influence on function by inhibiting neurotransmitter release. However, under different circumstances or at different doses the same opioids are also excitatory (12, 27). This dual capacity is evident in heart when enkephalins are introduced into the sinoatrial (SA) node by microdialysis during vagal stimulation. At femtomolar infusion rates rates, methionine-enkephalin-arginine-phenylalanine (MEAP) facilitates vagal transmission and lowers heart rate while at higher picomolar infusion rates in the same animal, MEAP interrupts vagal transmission and raises heart rate (10, 12, 18). In this instance, the vagotonic of MEAP effect was blocked by the DOR-1 receptor antagonist, BNTX and was duplicated by the DOR-1 agonist TAN-67 (8, 27). In contrast, the vagolytic effect was blocked by the DOR-2 antagonist, naltriben and duplicated by the DOR-2 agonist, deltorphin (11, 12).

Repeated occlusion of the SA node artery increased the endogenous MEAP recovered by microdialysis. Contrary to initial expectations, when vagal transmission was tested after completing the preconditioning, a clear vagotonic effect was observed but only during arterial occlusion when interstitial MEAP was elevated (19). The vagotonic effect observed during those late occlusions was initially reversed by the general DOR antagonist naltrindole (19) and in later studies by the more selective DOR-1

antagonist, BNTX (12). The vagotonic effect of endogenous MEAP is consistent with the ease of achieving local tissue peptide concentrations in the femtomolar range (38). The role of the DOR-1 receptors in this process is likewise consistent with their purported role in ischemic preconditioning (31, 33). The opposing vagotonic and vagolytic effects of MEAP are however less easily explained since both responses are attributed to a single receptor transcript. The DOR-2 mediated vagolytic effect of deltorphin is very robust and easily demonstrated but the intensity of the response is reduced following pretreatment with the DOR-1 agonist, TAN-67 (8). The vagolytic response was also eroded following the introduction of the ganglioside, GM-1 a common constituent of membrane lipid rafts (7). These observations lead to a working hypothesis that opposing functional phenotypes of the DOR are coupled differently and that the coexisting phenotypes are exchangeable either directly or through a sublemmal pool of indifferent DORs.

The observed effects of administered opioids are proposed to result from the net effects of opposing excitatory and inhibitory influences (5, 29, 30). The relative strengths of these opposing influences were determined in part by the local opioid concentration and the membrane environment surrounding its receptor (5). Pretreatment of the SA node with the DOR-1 agonist, TAN-67 or the membrane ganglioside GM-1 both reduced the vagolytic effect of the DOR-2 agonist, deltorphin. Thus a decline in competing vagolytic influences might explain the apparent emergence of the observed vagotonic effect following the PC protocol.

The nodal artery preconditioning studies described above did not determine whether the vagotonic effect that followed the PC protocol was the result of the conditioning stimulus, the extended arterial occlusion or a combination of both. The study that follows was designed to resolve that question. After completing the PC protocol, a vagolytic dose of MEAP was administered under perfused and occluded conditions to test further whether the vagolytic effect remained intact or had it been eroded to unmask or enhance the observed vagotonic effect.

METHODS

All protocols were approved by the Institutional Animal Care and Use Committee and were in compliance with the NIH guide for the Care and Use of Laboratory Animals.

Surgical Preparation

Nineteen mongrel dogs of either gender weighing 15-25 kg were assigned at random to various experimental protocols. The animals were anesthetized with sodium pentobarbital (32.5 mg/kg), intubated and mechanically ventilated initially at 225 ml/min/kg with room air. Fluid filled catheters were inserted into the right femoral artery and vein and advanced into the descending aorta and inferior vena cava, respectively. The arterial line was attached to a Statham PD23XL pressure transducer to monitor heart rate and arterial pressure during the remainder of the surgical preparation. The venous line was used to administer supplemental anesthetic, as required. The acid-base balance and the blood gases were determined regularly with an Instrumental Laboratories Blood Gas Analyzer (Lexington, MA). The PO_2 (90-120 mmHg), the pH (7.35-7.45) and the PCO_2 (30-40 mmHg) were adjusted to normal by administering supplemental oxygen, bicarbonate or modifying the minute volume.

The right and left cervical vagus nerves were isolated through a ventral midline surgical incision. The nerves were double ligated with umbilical tape to prevent afferent nerve traffic during electrical stimulation. The isolated nerves were then returned to the

prevertebral compartment for later retrieval. Surgical anesthesia was carefully monitored, and a single dose of succinylcholine (50 μ g/kg) was administered intravenously to temporarily reduce involuntary movements of the thoracic muscles during the 10-15 minutes required for electrosurgical incision of the chest. The costosternal cartilage for ribs 2-5 were severed to permit access to the thoracic cavity and the heart was exposed from the right aspect. The pericardium was opened and the dorsal pericardial margins were sutured to the body wall to support the heart. The left femoral artery was isolated and a high fidelity catheter pressure transducer (Millar Instruments, Houston, TX) was inserted and advanced into the abdominal aorta to measure heart rate and blood pressure continuously thereafter online (ADI Instruments, Bella Vista NSW, Australia).

The SA node artery was identified as a branch of the right coronary artery and traced visually to the SA node. A suture was placed loosely around the SA node artery near its origin. The suture secured with a slipknot to permit the reversible occlusion of the SA node artery as required.

Nodal Microdialysis

The SA node was visualized at the junction of superior vena cava and the right atrium. A 25 gauge stainless steel needle containing a microdialysis line was inserted into the center of the sinoatrial node parallel with the long axis of the node (17, 35). The needle was removed and the probe was then positioned so that the dialysate window was completely within the substance of the sinoatrial node. The microdialysis probe was

constructed of a single 1cm length of dialysis fiber from a Clirans TAF08 (Asahi Medical, Tokyo, Japan) artificial kidney (200 μm ID, 220 μm OD) and hollow 170- μm OD silica glass fiber inflow and outflow lines (SGE, Austin TX). The dialysis tubing permits molecules with a molecular mass of 35,000 kDa or less to cross from the lumen into the nodal interstitium. This technique allows the precise introduction of agents directly into the nodal interstitium for extended periods without provoking complicating systemic reflexes. After placement of the probe in the SA node, the dialysis line was perfused with saline at a rate of 5 $\mu\text{l}/\text{min}$ for one hour while the preparation was allowed to equilibrate.

Materials

MEAP (methionine-enkephalin-arginine-phenylalanine) and BNTX (7-benzylidenaltrexone) were obtained respectively from American Peptide (Sunnyvale, CA) and Tocris Bioscience (Ellisville, MO).

Statistical Methods

All data were expressed as mean and standard error of mean. Differences within subjects were evaluated with repeated measures ANOVA and post hoc analysis was performed with Tukey's test (GB-STAT, Dynamic Microsystems, Silver Springs, MD) for multiple cross comparisons and Dunnett's test was used for multiple comparisons to control. Selected comparisons made between protocols were evaluated with aid of a simple ANOVA followed again by either Tukey's or Dunnett's test as appropriate. In all

cases, differences determined to occur by chance with a probability <0.05 were deemed statistically significant.

Protocol 1: Preconditioning protocol.

After equilibration, the right cervical vagus nerve was stimulated at a supra-maximal voltage (15 volts) for 15 seconds at 3 Hz. This frequency was selected to produce a reproducible decline in heart rate of 30-50 bpm. After the control vagal response the SA node artery was temporarily occluded five times for 10 min each in an PC protocol. After each occlusion the slipknot was released and the artery was perfused normally for 10 min before beginning the next occlusion. The effect of vagal stimulation on heart rate was evaluated by stimulating the right cervical vagus again at the end of the 1st, 3rd, and 5th occlusions just prior to releasing the slipknot as indicated by the vertical arrows in the protocol diagram (Figure 1). The stimulation times were selected to minimize the total number of stimulations and to evaluate the effect of occlusion at the beginning, middle and end of the PC protocol. The stimulation during the 5th occlusion corresponds in time to the stimulation following the IPC protocol at which the vagotonic effect was first observed in earlier studies (17). Control stimulations were conducted during the 4th and 5th reperfusions. After completing the PC protocol (cycle five), the effect of exogenous MEAP on vagal transmission was evaluated three times. MEAP was first added into the dialysis inflow immediately after completing reperfusion five. The dose rate and exposure (1nmole/min for 5 min) were based on prior studies (9, 17). The dose was selected from dose response data to produce a submaximal vagolytic effect of

near 90% of maximal inhibition and maximize the opportunity to observe a decrement in the vagolytic effect (16). After washing out the MEAP, the restoration of basal vagal transmission was verified. The MEAP infusion was then restarted and a 6th occlusion-reperfusion cycle was conducted during the exogenous MEAP administration to evaluate the vagolytic effect in succession during both occlusion and reperfusion. The vagal-heart rate response was evaluated again before releasing the occlusion and then again after ten min of reperfusion. The MEAP was discontinued and washed out for 30 min. The restoration of basal vagal transmission was verified after the washout interval.

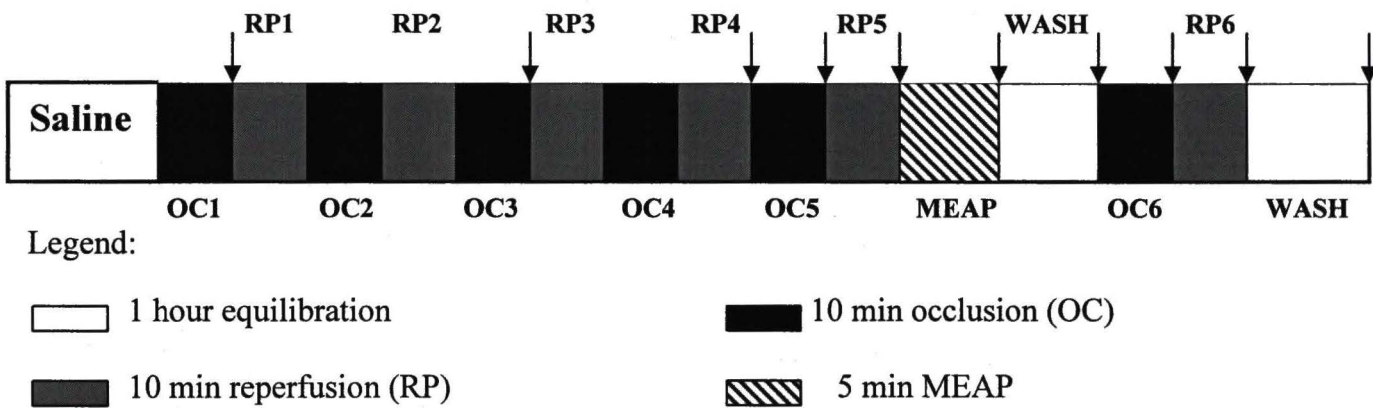


Figure: The figure summarizes the linear sequence of events during experimental Protocol 1. The arrows indicate the times when the right vagus nerve was stimulated.

Protocol 2: Sham Preconditioning Protocol (Time control).

The purpose of study two was to determine the potential influence of the duration of the protocol or the repeated vagal stimulation on the subsequent vagal transmission and/or its response to exogenous MEAP. Protocol 2 was identical to protocol 1 except the suture was not tightened at the times corresponding to occlusions 1 through 4 creating a sham PC protocol. Two variants of the protocol were conducted one with and one

without an occlusion during stimulation five. The MEAP infusions and subsequent occlusion six were identical to protocol 1.

Protocol 3: DOR-1 blockade with BNTX prevents the preconditioning effect.

The purpose of study three was to determine the potential role of the DOR-1 in the developing vagotonic response and any subsequent changes in the vagolytic, DOR-2 response. Protocol 3 was repeated as described above for protocol 1, except that the specific DOR-1 antagonist, BNTX (1 nmole/min) was introduced into the perfusate before the beginning the PC protocol and was maintained in the perfusate throughout the remainder of the PC protocol and post-PC protocol. The dose of BNTX employed was supramaximal based on the relative efficacy and selectivity of BNTX versus the vagotonic effect of MEAP in this model system (12).

RESULTS

Baseline Cardiovascular Indices: Table 1 summarizes the resting heart rate and blood pressure throughout each of the three protocols. There was no difference in the initial measure between groups nor was there change in either variable during the course of any of the three protocols. The apparent trend toward a higher heart rate in the BNTX group was well within historical norms for this model and was not the result of the DOR-1 blockade.

Study 1a PC Protocol: Figure 1 illustrates the changes in heart rate observed when the right vagus nerve was stimulated at 3 Hz at the beginning, middle and end of the IPC protocol. As demonstrated by others (19), the series of four short nodal artery occlusions and reperfusion increased the effect of vagal stimulation during the later 5th occlusion. This improvement in nodal vagal transmission clearly required time and/or multiple occlusions to develop since it was not evident after the 1st occlusion but had emerged by the end of the 3rd occlusion. Occlusion alone is thus not sufficient to demonstrate the vagotonic effect. The vagal response observed during the 4th reperfusion was similar to the initial control response. The near restoration of this control response confirms further that the vagotonic response is specifically observed when nodal blood flow is compromised. Contrary to that observation, the stimulation during reperfusion

five (after the 5th occlusion) persisted longer suggesting a greater opioid accumulation with successive occlusions and/or a slower washout.

Study 1b Sham PC Protocol: Figures 2(a) and 2(b) illustrate the changes in heart rate in two sham groups in which the vagus was stimulated sequentially without conducting any prior nodal arterial occlusions. The crosshatch bars represent stimulations performed at times equivalent to those conducted during occlusions in the prior study. The vagally mediated change in heart rate at each sham occlusion was not different from control stimulations and thus vagal efficacy was unaltered by time or repeated vagal stimulation. In the second group (Figure 2b), a single occlusion was conducted at a time equivalent to occlusion five to evaluate the combined effect of repeated stimulation, elapsed time and occlusion. The vagal efficiency of that single late occlusion was not different from the preceding or subsequent sham, non-occluded stimulations. Thus, there was no vagotonic effect in the absence of preceding occlusions.

Study 1c PC Protocol and DOR-1 blockade: Figure 3 illustrates the changes in heart rate observed when the right vagus nerve was stimulated at 3 Hz at selected times during the PC protocol in the presence of DOR-1 blockade with BNTX. The control response illustrated in the figure was conducted prior to adding BNTX to the dialysate. BNTX itself produced a small but non-significant increase in the response to vagal stimulation (not shown). The results of the subsequent stimulations during the 1st, 3rd, and 5th occlusions were not different from control. Heart rate responses during reperfusion five

and six were likewise not different from control. Thus, blockade of the DOR-1 produced a vagal response pattern during the IPC protocol that is indistinguishable from the unoccluded time control (Figures 2a, 2b) confirming that the vagotonic response is DOR-1 dependent.

Study 2a PC and Exogenous MEAP: Study 2 was designed to test whether the vagotonic responses observed during the PC protocol might arise from a reduction in opposing DOR-2 mediated vagolytic responses. As illustrated in Figure 4, a submaximal dose of MEAP was tested to insure a sufficient reserve in which to observe a reduction in the vagolytic response. After completing the five cycle PC protocol, MEAP was tested prior to occlusion. Since the PC protocol produced an increase in vagal efficacy, the degree of inhibition observed was dependent on which control was used. MEAP produced a calculated 21% reduction in the vagal response compared to the original control from the start of the experiment. If the post-washout control were used, the degree of inhibition was closer to 34% for the post-PC control. The MEAP was washed out and restoration of the post-PC-control response was demonstrated. When the nodal artery was occluded for a 6th time and MEAP was added back to the dialysis inflow, the effect of vagal stimulation was reduced further from 21% to 13% of the original control. In order to determine whether the perceived loss of efficacy during occlusion was specific to the occlusion, the MEAP was continued, the slipknot was released and the vagus was reevaluated 10 min later. Surprisingly, the vagolytic response of MEAP was reduced further yet from 13% to 0% and the rate of attrition seemed to have accelerated.

The MEAP was discontinued and the restoration of the vagal response was demonstrated after 10 min. The percent changes were smaller if calculated from the post-PC washout however the progressive pattern of attrition was identical.

Study 2b Sham IPC Protocol and Exogenous MEAP: Figure 5a and 5b illustrate the results of the MEAP evaluations following the sham-PC protocols in the presence and absence of occlusions during OC5. In the absence of prior PC occlusions, MEAP reduced the vagal bradycardia by 62% similar to the historical effect of MEAP in non-occluded animals. The vagal response was fully restored following washout. When the MEAP was combined with an initial occlusion, the magnitude of the vagolytic effect was again reduced, in this case from 62% to 47%. The MEAP was continued and the nodal artery occlusion was released. The subsequent vagal stimulation after 10 min reperfusion with continued MEAP revealed a continued erosion of the vagolytic response from 47% to 39%. Once again washout fully restored the control vagal response. Although the declining vagolytic effects were less complete following the sham-PC protocol, the pattern of attrition was very similar to that after PC.

In order to evaluate the effects of prior occlusion on the vagolytic response of MEAP, the post-PC protocol was repeated in the late occlusion shams. Following the single occlusion at interval five, MEAP reduced the vagal bradycardia by 45% as compared to 62% in the absence of that occlusion. The vagolytic effect of MEAP declined further to 23% during the subsequent (second) occlusion suggesting an

interaction between occlusion and MEAP. Following the release of the occlusion temporally equivalent to RP6, the MEAP response was reduced further (13% vs 39%) compared to the post-PC sham with only one occlusion supporting further an interaction between occlusion and MEAP to down regulate the DOR-2 response.

Study 2c PC, DOR-1 blockade and MEAP: Figure 6 illustrates the results of the MEAP evaluations following the PC in the presence of DOR-1 blockade throughout the protocol. The post-PC vagolytic effect of MEAP was very weak, similar to that observed after PC in the absence of BNTX. Following PC + BNTX, MEAP reduced the vagally mediated decline in heart rate by only 19%. Washing out the MEAP once again restored the vagally mediated bradycardia to control conditions. Reintroducing MEAP during nodal artery occlusion reduced the vagolytic influence of MEAP from 19% to 8%. When rechecked again 10 min later during reperfusion, the vagolytic influence of MEAP was nearly eliminated at 3%. After washing out the MEAP, vagal stimulation produced a decline in heart rate that was again not different from control.

Study 2d Vagolytic Effects, Cross Study Comparisons: The initial 62% inhibition of vagally mediated bradycardia by MEAP in the sham was consistent with the 60-75% inhibition typically observed (4, 9-11, 18) indicating that time or repeated stimulation does not erode the vagolytic response. The 21-34% inhibition by MEAP observed after completing the PC protocol suggests that MEAP was now less effective compared with the Sham-PC (21% vs 62%, $P < 0.5$). MEAP remained inhibitory when administered

during the occlusion in all three studies though the magnitude of that effect was less in the two PC studies during occlusion (47% vs 13% vs 8%, $P < 0.05$) and again during the subsequent reperfusion (39% vs 0% vs 3% $p < 0.05$). Occlusion itself also may reduce the efficacy of MEAP.

DISCUSSION

Individuals with strong parasympathetic control of the heart generally have better prognoses following adverse cardiovascular events. Those who recover vagally mediated heart rate variability quickly after myocardial infarction are much more likely to survive (21). Carotid massage acutely increases efferent parasympathetic traffic and is routinely employed to modify selected cardiac arrhythmias. Exercise training chronically increases parasympathetic influences on heart rhythms and reduces both myocardial damage and the incidence of ventricular fibrillation after coronary occlusion (1-3). In contrast, inappropriate or intense parasympathetic activity can reduce the refractory period and facilitate the genesis of abnormal rhythms. Thus, the nuances of vagal transmission and the factors that modulate its plasticity are important targets for investigation.

Cardiac enkephalins (16, 23, 34) and the associated DOR are capable of dramatically modifying parasympathetic transmission at the vagal, myocardial interface. Although the opioids are traditionally viewed as exerting their influence by inhibition of neurotransmitter release, excitatory effects of opioids are routinely observed in many systems (29). Nanomolar doses of MEAP administered by dialysis into the interstitium of the SA node interrupted vagal transmission. The DOR-2 antagonist, naltriben selectively blocked this vagolytic influence. Femtomolar doses of MEAP in contrast increased the efficacy of vagal stimulation (12). Applying an IPC protocol to the nodal

artery produced similar femtomolar increases in MEAP in the nodal interstitium. An improved vagal transmission was observed afterward only during subsequent occlusions when MEAP was elevated. Both of these vagotonic effects were abrogated by sub-femtomolar infusions of the DOR-1 antagonist, BNTX. The original four-cycle PC studies did not test whether the late occlusion alone, the prior PC protocol or both were both required to demonstrate the vagotonic effect.

The results obtained in the current study suggest that occlusion alone was not sufficient to produce an immediate vagotonic effect since no change in vagal efficacy was observed during the 1st occlusion. Graded improvements in vagal transmission were observed during the 3rd and 5th occlusions suggesting that the capability evolves over time. Whether the vagotonic response requires multiple occlusions or simply a single trigger occlusion to initiate the process followed by sufficient time for the vagotonic response to evolve remains unclear. However, the late occlusion performed during sham experiments clearly demonstrated that there was no improvement in the vagal function due to a single occlusion and a longer protocol is required to generate the vagotonic effect.

The prior pharmacologic studies of DOR interactions in the canine SA node have suggested that the proportion of functioning DOR-1 and DOR-2 phenotypes can be fluid and the sum of their opposing influences determine the net effect observed at any point in time. The PC mediated emergence of the vagotonic phenotype during the later

occlusions in the PC protocol might thus represent an increase in DOR-1 influence and/or a reduction in the DOR-2 influence. The emerging vagotonic effect was clearly DOR-1 mediated throughout the five-occlusion protocol since DOR-1 blockade with BNTX eliminated the improved vagal transmission.

The PC protocol also reduced the DOR-2 mediated vagolytic influence of added MEAP during both perfusion and occlusion. Historically, MEAP inhibits vagal transmission by 60-75% as observed in the time controls from this study. The initial 21%-34% inhibition of vagal transmission observed after PC was lower than expected during normal perfusion. The vagolytic effect of added MEAP declined progressively during the subsequent occlusion and reperfusion nearly disappearing during the final evaluation. The PC protocol clearly contributes to the DOR-2 decline which was much less complete in time controls. MEAP alone did not dramatically reduce its own vagolytic response even when repeatedly applied during normal perfusion (9). Thus, the decline in the DOR-2 response appears to be more complicated than simple homologous desensitization. PC appears to mediate a change in the receptor environment that favors down regulation of the DOR-2 response.

The studies discussed above sought to test the primary hypothesis that PC was responsible for the appearance of vagotonic effects. The second hypothesis sought to test whether PC reduced competing vagolytic effects. The analyses above suggest that both are correct; PC improves DOR-1 mediated vagotonic responses and accelerates the

disappearance of DOR-2 mediated vagolytic responses. The hypothesis was formulated from previous studies that showed repeated SA node arterial occlusions raised endogenous opioids and produced corresponding improvement in the vagal function (12, 19). Whether these DOR mediated interactions with vagal transmission are in integral part of cardioprotective mechanisms or a convenient bioassay of DOR status remains open for discussion. Very little is known about the preconditioning effects on the right side of the heart, however a functional shift of DOR-2 to DOR-1 mediated responses would presumably be beneficial since the DOR-1 is the putative cardioprotective phenotype (22, 31, 32).

The third experiment was designed to verify the DOR-1 character of the evolving vagotonic response and to test the hypothesis that PC mediated DOR-1 stimulation was responsible for the subsequent erosion and elimination of the DOR-2 vagolytic effect. BNTX completely prevented the PC mediated vagotonic effect indicating its mediation by DOR-1 receptors. This dose of BNTX was previously determined as ineffective against DOR-2 mediated responses (12). Contrary to the hypothesis, the subsequent challenges with added MEAP produced very weak vagolytic responses that quickly disappeared during sequential exposures. The rate of attrition in the response was nearly identical to the pattern observed after PC alone. PC appears to facilitate the loss of the vagolytic response independently of its DOR-1 receptor stimulation. This is inconsistent with prior results in which DOR-1 stimulation with the selective DOR-1 agonist TAN-67 increased the rate of decline in DOR-2 responses (8). These conflicting observations

would be compatible if the extended exposure to BNTX alters receptor trafficking. Thus, the PC mediated vagotonic response is DOR-1 mediated but role of that DOR-1 receptor stimulation in the PC mediated decline in the DOR-2 response is unresolved.

Integrating the current findings with prior work supports a unifying hypothesis that intermittent metabolic stress increases local myocardial enkephalin production that then easily activates the more sensitive DOR-1 receptors on nearby vagal processes (12). The DOR-1 receptor stimulates adenylyl cyclase activity in the prejunctional terminals through a GM-1, $G_{S\alpha}$ -dependent coupling mechanism that increases calcium influx, vesicular transport and acetylcholine release (5, 20, 36). DOR-1 mediated increases in protein kinase A (PKA) increase GM-1 synthesis. The increased plasma membrane GM-1 completes a positive feedback loop by recruiting indifferent DORs into the DOR-1 phenotype as they emerge into the plasma membrane from the sublemmal compartment. Thus, GM-1 increases the probability that emerging DORs assume the DOR-1 configuration. The hypothesis proposes further that $G_{i\alpha}$ and the inhibition of adenylyl cyclase activity mediate the vagolytic action of DOR-2 stimulation (14, 30). DOR-2 stimulation also dramatically increases the exchange of receptor between surface and cytoplasm (6, 8, 24). When GM-1 is available, the DOR-2 stimulated trafficking of receptors favors the exchange of existing DOR-2 for new DOR-1. This is consistent with both the DOR-1 and GM-1 mediated erosion of DOR-2 responses reported previously (7, 8).

The loss of the DOR-2 response following extended exposure to BNTX would be consistent with the trafficking hypothesis if BNTX sequesters the emerging receptors on the surface and removes them from the exchangeable circulating pool. The declining pool of receptors would quickly deplete those available for either phenotype. Thus, the extended DOR-1 blockade eliminates all vagotonic influences directly and a rapidly depletes the recycling pool of indifferent receptors available to mediate DOR-2 vagolytic responses.

Experimental cardiac preconditioning often employs transient arterial occlusions or added opioids active at the DOR-1 receptor. Thus, understanding how to manipulate the proportion of DOR-1 and DOR-2 receptors could be valuable for inducing a cardioprotective phenotype with a favorable DOR mix.

In conclusion, the vagotonic result observed during arterial occlusion requires preconditioning for complete expression and could result in part from reduced competition from vagolytic effects. BNTX abolished the vagotonic effects of preconditioning confirming DOR-1 participation. BNTX also reduced the vagolytic effects of MEAP during occlusion and reperfusion supporting a complex interplay between DOR-1 and DOR-2 trafficking.

REFERENCES

1. **Billman GE, Schwartz PJ and Stone HL.** The effects of daily exercise on susceptibility to sudden cardiac death. *Circulation* 69: 6: 1182-1189, 1984.
2. **Binkley PF, Nunziata E, Haas GJ, Nelson SD and Cody RJ.** Parasympathetic withdrawal is an integral component of autonomic imbalance in congestive heart failure: demonstration in human subjects and verification in a paced canine model of ventricular failure. *J.Am.Coll.Cardiol.* 18: 2: 464-472, 1991.
3. **Brown DA and Moore RL.** Perspectives in innate and acquired cardioprotection: cardioprotection acquired through exercise. *J.Appl.Physiol.* 103: 5: 1894-1899, 2007.
4. **Caffrey JL, Mateo Z, Napier LD, Gaugl JF and Barron BA.** Intrinsic cardiac enkephalins inhibit vagal bradycardia in the dog. *Am.J.Physiol.* 268: 2 Pt 2: H848-55, 1995.
5. **Crain SM and Shen KF.** After chronic opioid exposure sensory neurons become supersensitive to the excitatory effects of opioid agonists and antagonists as occurs after acute elevation of GM1 ganglioside. *Brain Res.* 575: 1: 13-24, 1992.
6. **Cvejic S and Devi LA.** Dimerization of the delta opioid receptor: implication for a role in receptor internalization. *J.Biol.Chem.* 272: 43: 26959-26964, 1997.

7. **Davis S, Deo SH, Barlow M, Yoshishige D, Farias M and Caffrey JL.** The monosialosyl ganglioside GM-1 reduces the vagolytic efficacy of delta2-opioid receptor stimulation. *Am.J.Physiol.Heart Circ.Physiol.* 291: 5: H2318-26, 2006.
8. **Deo SH, Johnson-Davis S, Barlow MA, Yoshishige D and Caffrey JL.** Repeated delta1-opioid receptor stimulation reduces delta2-opioid receptor responses in the SA node. *Am.J.Physiol.Heart Circ.Physiol.* 291: 5: H2246-54, 2006.
9. **Farias M,3rd, Jackson K, Johnson M and Caffrey JL.** Cardiac enkephalins attenuate vagal bradycardia: interactions with NOS-1-cGMP systems in canine sinoatrial node. *Am.J.Physiol.Heart Circ.Physiol.* 285: 5: H2001-12, 2003.
10. **Farias M,3rd, Jackson KE, Yoshishige D and Caffrey JL.** Cardiac enkephalins interrupt vagal bradycardia via delta 2-opioid receptors in sinoatrial node. *Am.J.Physiol.Heart Circ.Physiol.* 284: 5: H1693-701, 2003.
11. **Farias M, Jackson K, Stanfill A and Caffrey JL.** Local opiate receptors in the sinoatrial node moderate vagal bradycardia. *Auton.Neurosci.* 87: 1: 9-15, 2001.
12. **Farias M, Jackson K, Yoshishige D and Caffrey JL.** Bimodal delta-opioid receptors regulate vagal bradycardia in canine sinoatrial node. *Am.J.Physiol.Heart Circ.Physiol.* 285: 3: H1332-9, 2003.
13. **Goto M, Liu Y, Yang XM, Ardell JL, Cohen MV and Downey JM.** Role of bradykinin in protection of ischemic preconditioning in rabbit hearts. *Circ.Res.* 77: 3: 611-621, 1995.

14. **Grady EF, Bohm SK and Bunnett NW.** Turning off the signal: mechanisms that attenuate signaling by G protein-coupled receptors. *Am.J.Physiol.* 273: 3 Pt 1: G586-601, 1997.
15. **Gross GJ.** Role of opioids in acute and delayed preconditioning. *J.Mol.Cell.Cardiol.* 35: 7: 709-718, 2003.
16. **Howells RD, Kilpatrick DL, Bailey LC, Noe M and Udenfriend S.** Proenkephalin mRNA in rat heart. *Proc.Natl.Acad.Sci.U.S.A.* 83: 6: 1960-1963, 1986.
17. **Jackson K, Farias M and Caffrey JL.** Cardiac microdialysis a powerful tool. *Cardiovasc.Res.* 46: 3: 367-369, 2000.
18. **Jackson KE, Farias M, Stanfill A and Caffrey JL.** Delta opioid receptors inhibit vagal bradycardia in the sinoatrial node. *J.Cardiovasc.Pharmacol.Ther.* 6: 4: 385-393, 2001.
19. **Jackson KE, Farias M, Stanfill AS and Caffrey JL.** Transient arterial occlusion raises enkephalin in the canine sinoatrial node and improves vagal bradycardia. *Auton.Neurosci.* 94: 1-2: 84-92, 2001.
20. **Keren O, Gafni M and Sarne Y.** Opioids potentiate transmitter release from SK-N-SH human neuroblastoma cells by modulating N-type calcium channels. *Brain Res.* 764: 1-2: 277-282, 1997.

21. **Kleiger RE, Miller JP, Bigger JT, Jr and Moss AJ.** Decreased heart rate variability and its association with increased mortality after acute myocardial infarction. *Am.J.Cardiol.* 59: 4: 256-262, 1987.
22. **Kuzume K, Wolff RA, Amakawa K, Kuzume K and Van Winkle DM.** Sustained exogenous administration of Met5-enkephalin protects against infarction in vivo. *Am.J.Physiol.Heart Circ.Physiol.* 285: 6: H2463-70, 2003.
23. **Lang RE, Hermann K, Dietz R, Gaida W, Ganten D, Kraft K and Unger T.** Evidence for the presence of enkephalins in the heart. *Life Sci.* 32: 4: 399-406, 1983.
24. **Loh HH and Smith AP.** Molecular characterization of opioid receptors. *Annu.Rev.Pharmacol.Toxicol.* 30: 123-147, 1990.
25. **Mullane K and Bullough D.** Harnessing an endogenous cardioprotective mechanism: cellular sources and sites of action of adenosine. *J.Mol.Cell.Cardiol.* 27: 4: 1041-1054, 1995.
26. **Murry CE, Jennings RB and Reimer KA.** Preconditioning with ischemia: a delay of lethal cell injury in ischemic myocardium. *Circulation* 74: 5: 1124-1136, 1986.
27. **Portoghese PS, Sultana M, Nagase H and Takemori AE.** A highly selective delta 1-opioid receptor antagonist: 7-benzylidenenaltrexone. *Eur.J.Pharmacol.* 218: 1: 195-196, 1992.

28. **Przyklenk K, Darling CE, Dickson EW and Whittaker P.** Cardioprotection 'outside the box'--the evolving paradigm of remote preconditioning. *Basic Res. Cardiol.* 98: 3: 149-157, 2003.
29. **Sarne Y, Fields A, Keren O and Gafni M.** Stimulatory effects of opioids on transmitter release and possible cellular mechanisms: overview and original results. *Neurochem.Res.* 21: 11: 1353-1361, 1996.
30. **Schallmach E, Steiner D and Vogel Z.** Adenylyl cyclase type II activity is regulated by two different mechanisms: implications for acute and chronic opioid exposure. *Neuropharmacology* 50: 8: 998-1005, 2006.
31. **Schultz JE, Hsu AK and Gross GJ.** Ischemic preconditioning in the intact rat heart is mediated by delta1- but not mu- or kappa-opioid receptors. *Circulation* 97: 13: 1282-1289, 1998.
32. **Schultz JE, Hsu AK and Gross GJ.** Morphine mimics the cardioprotective effect of ischemic preconditioning via a glibenclamide-sensitive mechanism in the rat heart. *Circ.Res.* 78: 6: 1100-1104, 1996.
33. **Schultz JE, Rose E, Yao Z and Gross GJ.** Evidence for involvement of opioid receptors in ischemic preconditioning in rat hearts. *Am.J.Physiol.* 268: 5 Pt 2: H2157-61, 1995.

34. **Springhorn JP and Claycomb WC.** Translation of heart preproenkephalin mRNA and secretion of enkephalin peptides from cultured cardiac myocytes. *Am.J.Physiol.* 263: 5 Pt 2: H1560-6, 1992.
35. **Van Wylen DG, Willis J, Sodhi J, Weiss RJ, Lasley RD and Mentzer RM,Jr.** Cardiac microdialysis to estimate interstitial adenosine and coronary blood flow. *Am.J.Physiol.* 258: 6 Pt 2: H1642-9, 1990.
36. **Whistler JL, Tsao P and von Zastrow M.** A phosphorylation-regulated brake mechanism controls the initial endocytosis of opioid receptors but is not required for post-endocytic sorting to lysosomes. *J.Biol.Chem.* 276: 36: 34331-34338, 2001.
37. **Yao Z and Gross GJ.** Acetylcholine mimics ischemic preconditioning via a glibenclamide-sensitive mechanism in dogs. *Am.J.Physiol.* 264: 6 Pt 2: H2221-5, 1993.
38. **Younes A, Pepe S, Barron BA, Spurgeon HA, Lakatta EG and Caffrey JL.** Cardiac synthesis, processing, and coronary release of enkephalin-related peptides. *Am.J.Physiol.Heart Circ.Physiol.* 279: 4: H1989-98, 2000.
39. **Younes A, Pepe S, Yoshishige D, Caffrey JL and Lakatta EG.** Ischemic preconditioning increases the bioavailability of cardiac enkephalins. *Am.J.Physiol.Heart Circ.Physiol.* 289: 4: H1652-61, 2005.

LEGENDS

Figure 1: The figure illustrates changes in heart rate mediated by right vagal nerve stimulation at 3 Hz during the sequential occlusion and reperfusion of the PC protocol. Values are means and standard error of the mean for five subjects. The symbols (* and **) indicate the change in the heart rate was significantly different from control at $P < 0.05$ and $P < 0.01$ respectively.

Figure 2(a) and 2(b): Changes in heart rate mediated by repeated right vagus nerve stimulation are illustrated for sham occlusions. Stimulation intervals correspond to the periods of occlusion and reperfusion in Figure 1. Figure 2b includes a single occlusion corresponding to occlusion five. Values are means and standard error of the mean for five and four subjects respectively.

Figure 3: The figure illustrates the effect of DOR-1 blockade with BNTX on changes in heart rate mediated by right vagal nerve stimulation during the PC protocol. Values are means and standard error of the mean for five subjects.

Figure 4: Figure 4 illustrates the effects of MEAP administered by microdialysis into the SA node interstitium following completion of the PC protocol in Figure 1. The resulting changes in heart rate during right vagal stimulation are illustrated sequentially for MEAP

combined with reperfusion, occlusion and reperfusion. Values are means and standard error of the mean for five subjects. The symbols (* and **) indicate the change in the heart rate was significantly different from control at $P < 0.05$ and $P < 0.01$ respectively. The symbol (\$) indicates the change in the heart rate was significantly different from MEAP ($P < 0.05$).

Figure 5(a) and 5(b): The figures illustrate the effects of MEAP administered by microdialysis into the SA node interstitium following completion of the sham PC protocols in Figure 2a and 2b. The resulting changes in heart rate during right vagal stimulation are illustrated sequentially for MEAP combined with reperfusion, occlusion and reperfusion. Values are means and standard error of the mean for five and four subjects respectively. The symbols (* and **) indicate the change in the heart rate was significantly different from control at $P < 0.05$ and $P < 0.01$ respectively. The symbol (\$) indicates the change in the heart rate was significantly different from MEAP at $P < 0.05$.

Figure 6: Figure 6 illustrates the effects of DOR-1 blockade with BNTX on MEAP administered by microdialysis into the SA node interstitium following completion of the PC protocol in Figure 3. The resulting changes in heart rate during right vagal stimulation are illustrated sequentially for MEAP and BNTX combined with reperfusion, occlusion and reperfusion. Values are means and standard error of the mean for five subjects. The symbol (\$\$) indicates the change in the heart rate was significantly different from RP5 ($P < 0.01$).

TABLE 1: Resting Cardiovascular Indices:

Protocol 1: Preconditioning Protocol (n=5)									
	Control	OC1	OC3	RP4	OC5	RP5	MEAP	OC6	RP6
MAP (mmHg)	97 ±5	101 ±4	105 ±5	102 ±7	104 ±6	101 ±7	104 ±5	94 ±7	100 ±8
HR (bpm)	122 ±5	123 ±5	126 ±5	125 ±5	128 ±6	127 ±5	130 ±6	127 ±6	131 ±7
Protocol 2a: Controls: Vehicle and Duration (n=5)									
	Control	OC1	OC3	RP4	OC5	RP5	MEAP	OC6	RP6
MAP (mmHg)	95 ±4	95 ±5	99 ±4	104 ±3	102 ±4	97 ±4	96 ±4	99 ±1	105 ±6
HR (bpm)	124 ±7	121 ±6	120 ±6	120 ±7	119 ±7	118 ±7	116 ±6	115 ±7	116 ±7
Protocol 2b: Controls: Vehicle, Duration and OC5 (n=4)									
	Control	OC1	OC3	RP4	OC5	RP5	MEAP	OC6	RP6
MAP (mmHg)	105 ±2	103 ±2	104 ±2	106 ±2	103 ±0.4	103 ±2	107 ±1	108 ±2	109 ±1
HR (bpm)	129 ±4	124 ±5	119 ±5	110 ±7	110 ±5	109 ±7	108 ±7	106 ±5	107 ±6
Protocol 3: DOR-1 Mediate Preconditioning (n=5)									
	Control	OC1 + BNTX	OC3 + BNTX	RP4 + BNTX	OC5 + BNTX	RP5 + BNTX	MEAP + BNTX	OC6 + BNTX	RP6 + BNTX
MAP (mmHg)	98 ±7	92 ±7	95 ±5	97 ±3	95 ±5	94 ±4	99 ±3	94 ±6	98 ±3
HR (bpm)	144 ±9	140 ±9	140 ±8	138 ±9	135 ±9	132 ±11	134 ±8	136 ±8	139 ±8

Repeated SA Node Artery Occlusion Improves Vagotonic Responses

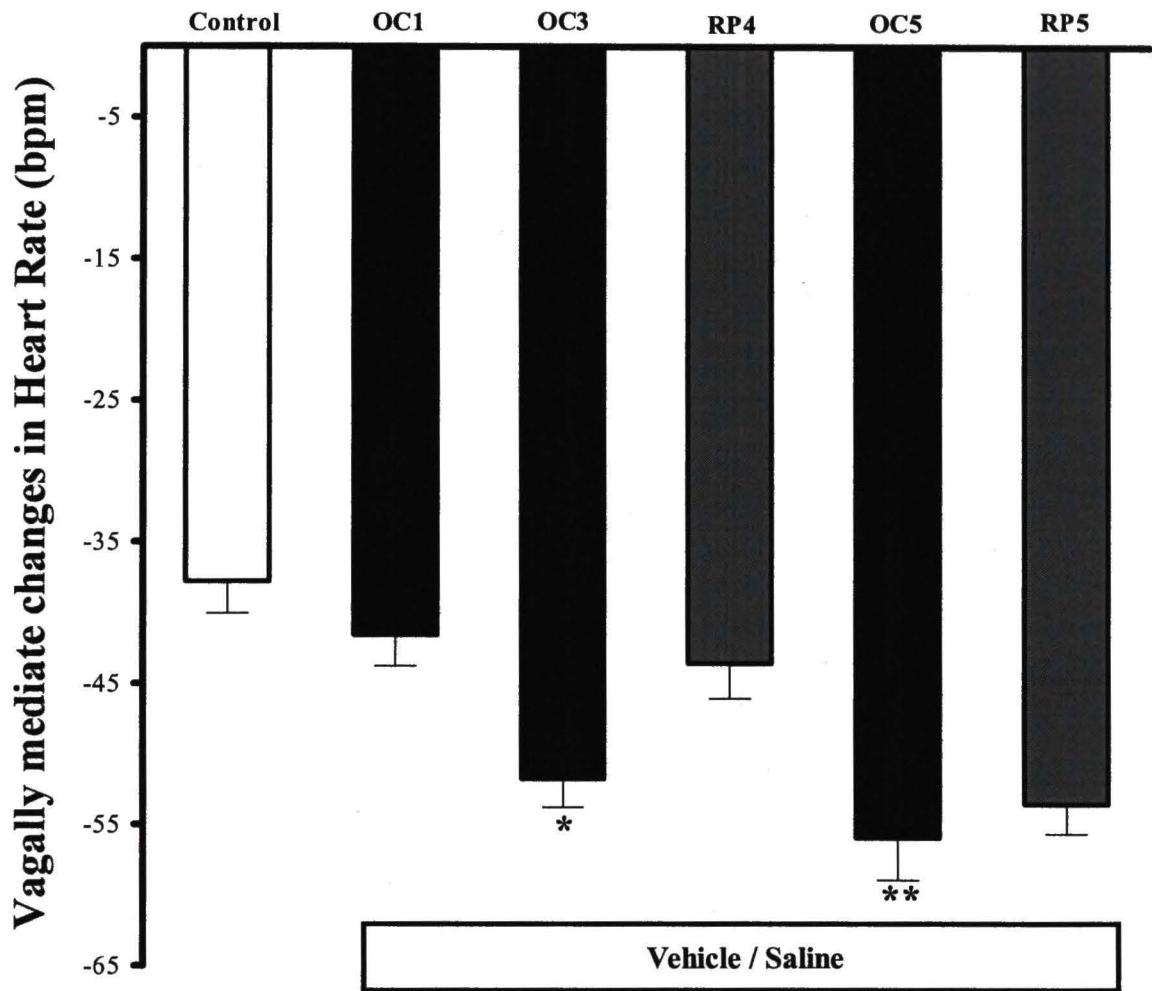


Figure 1

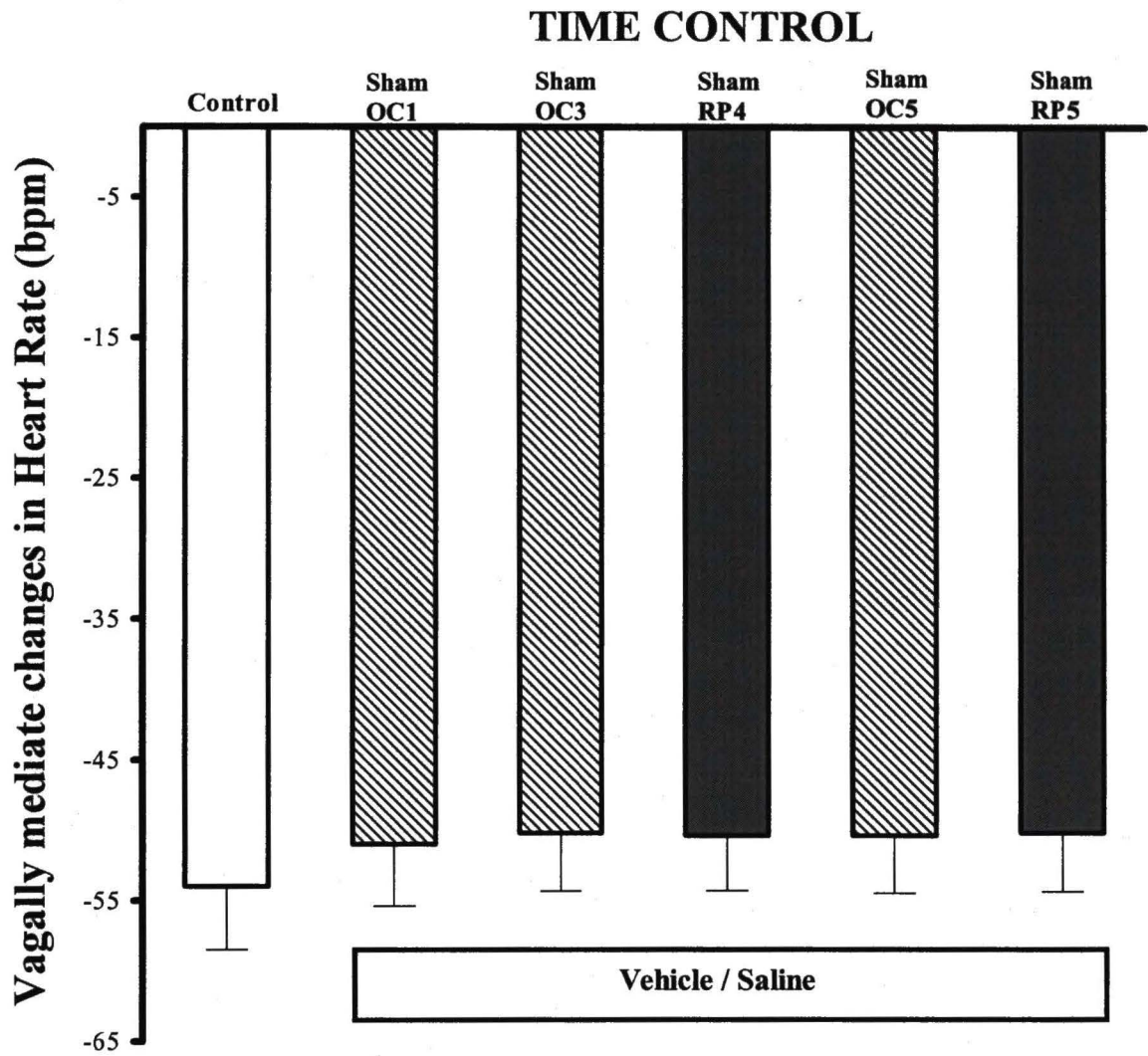


Figure 2(a)

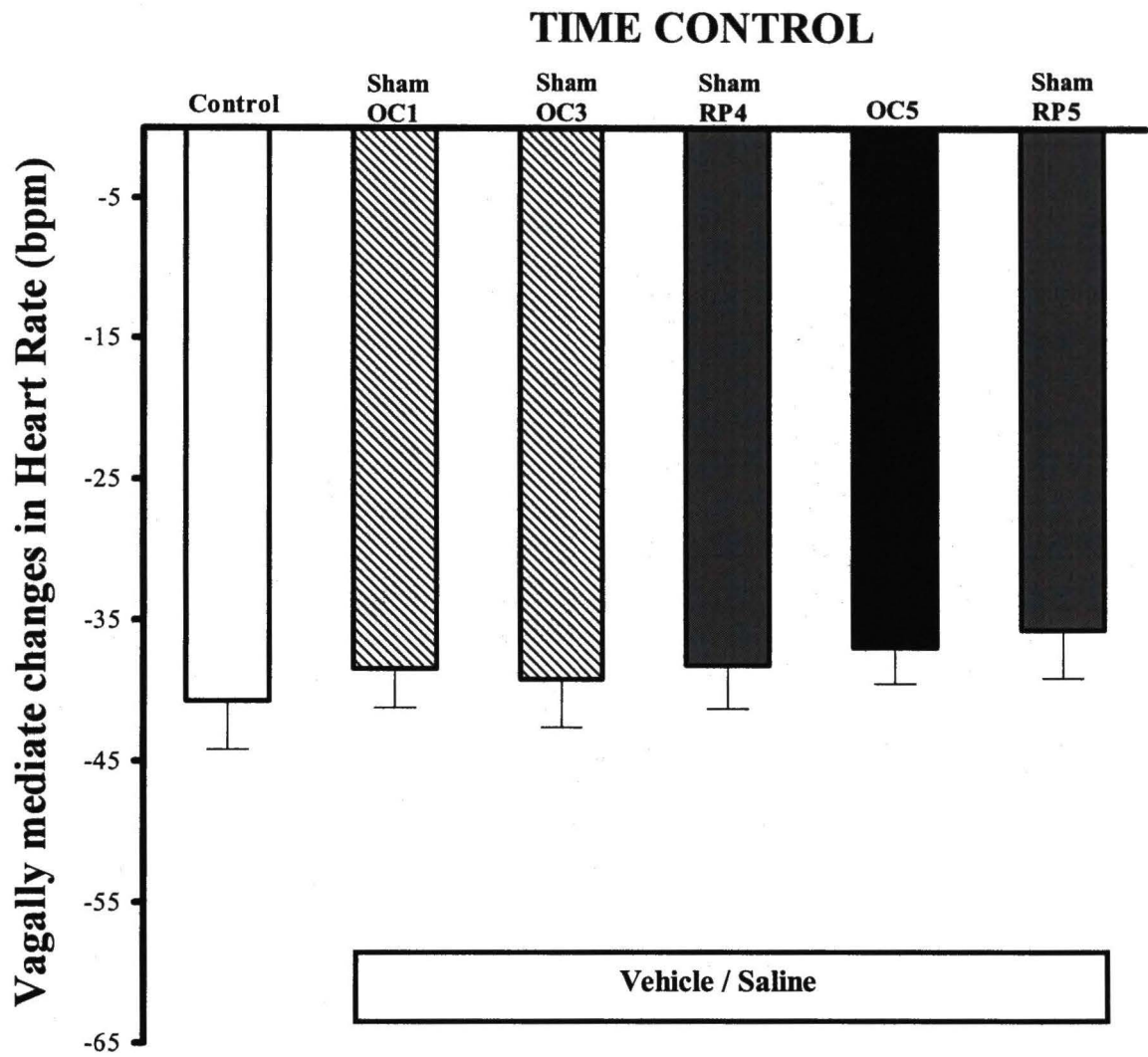


Figure 2(b)

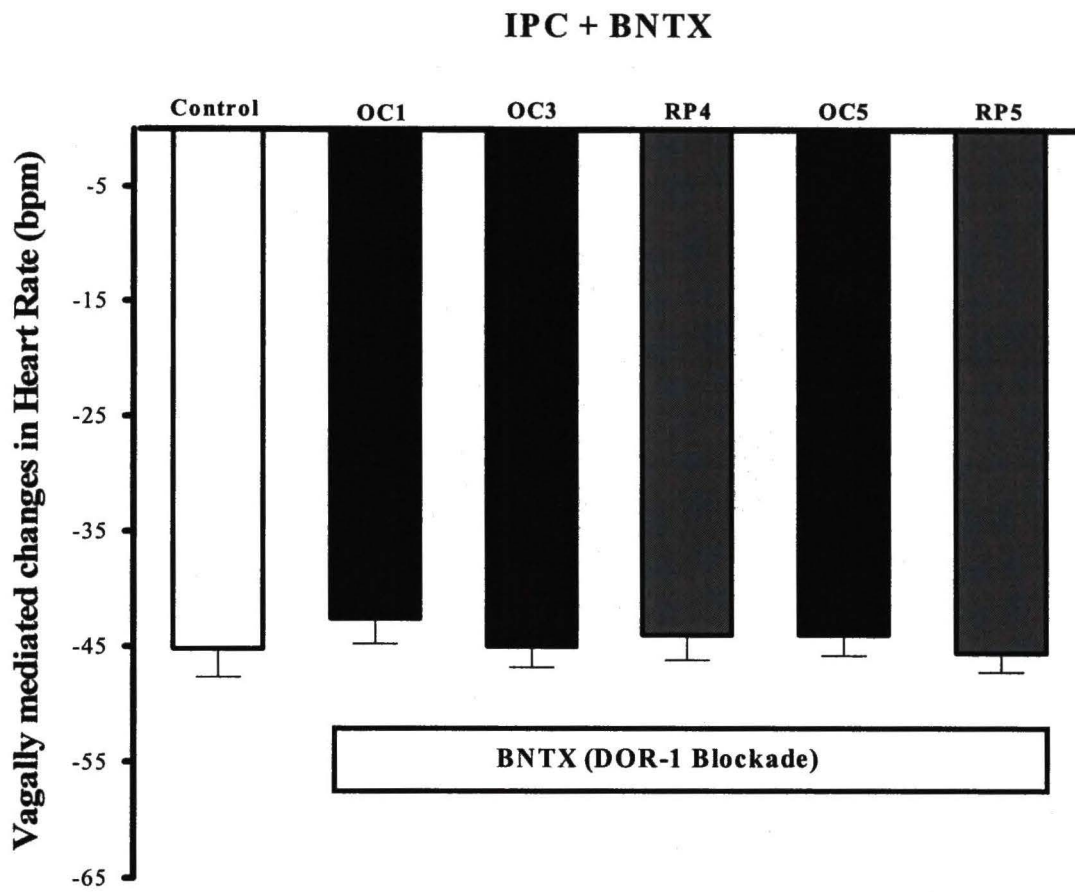


Figure 3

Repeated SA node Artery Occlusion Improves Vagotonic responses

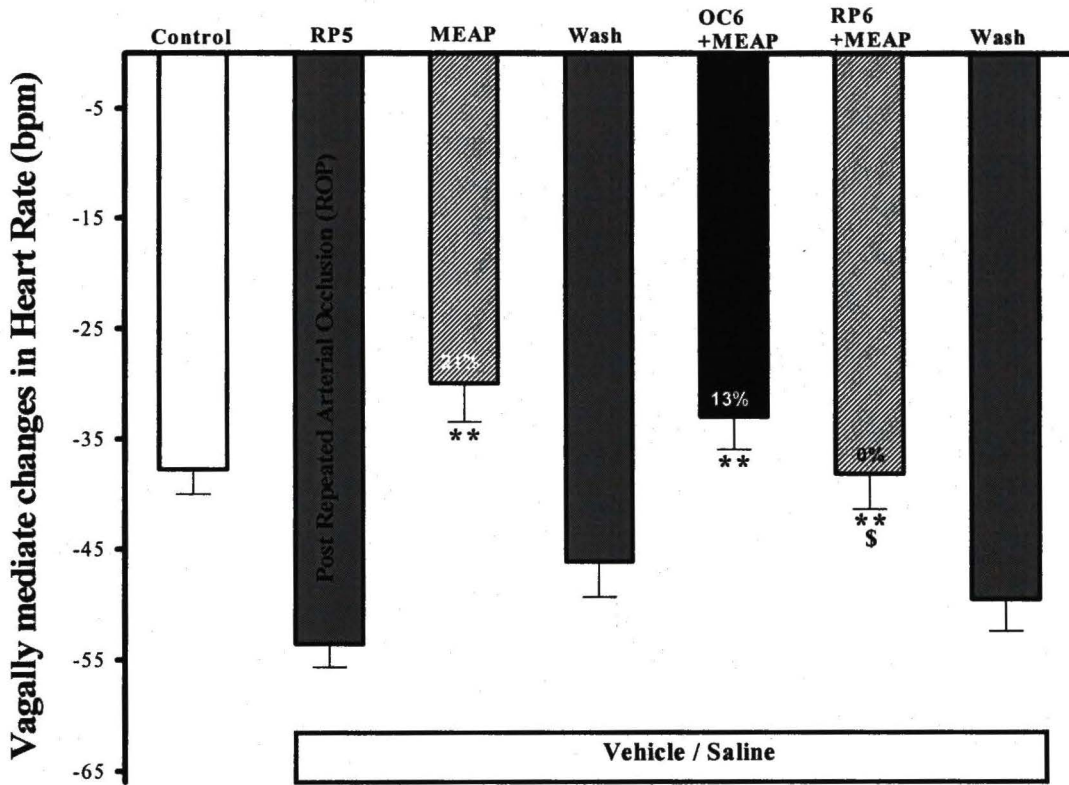


Figure 4

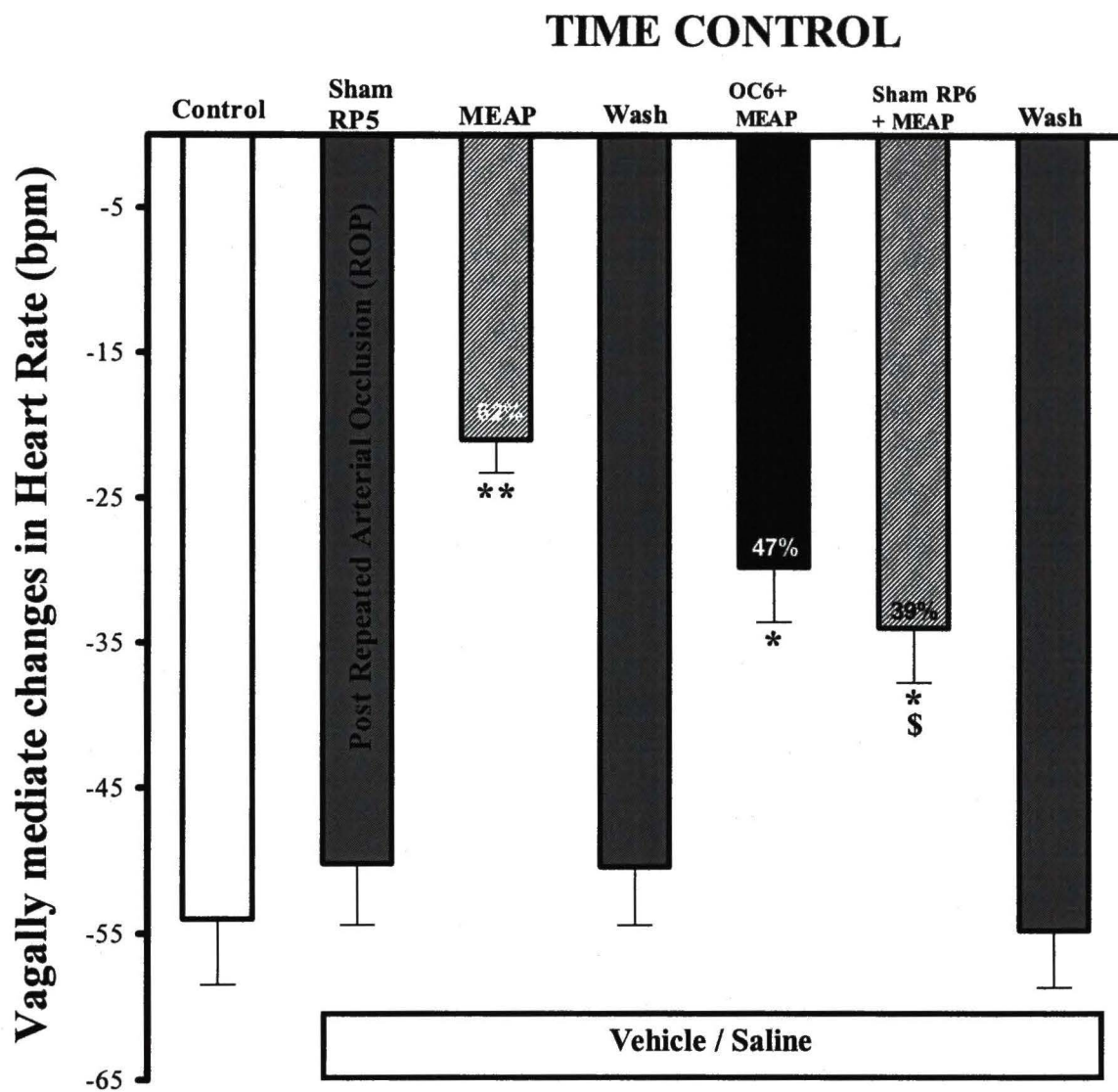


Figure 5(a)

TIME CONTROL

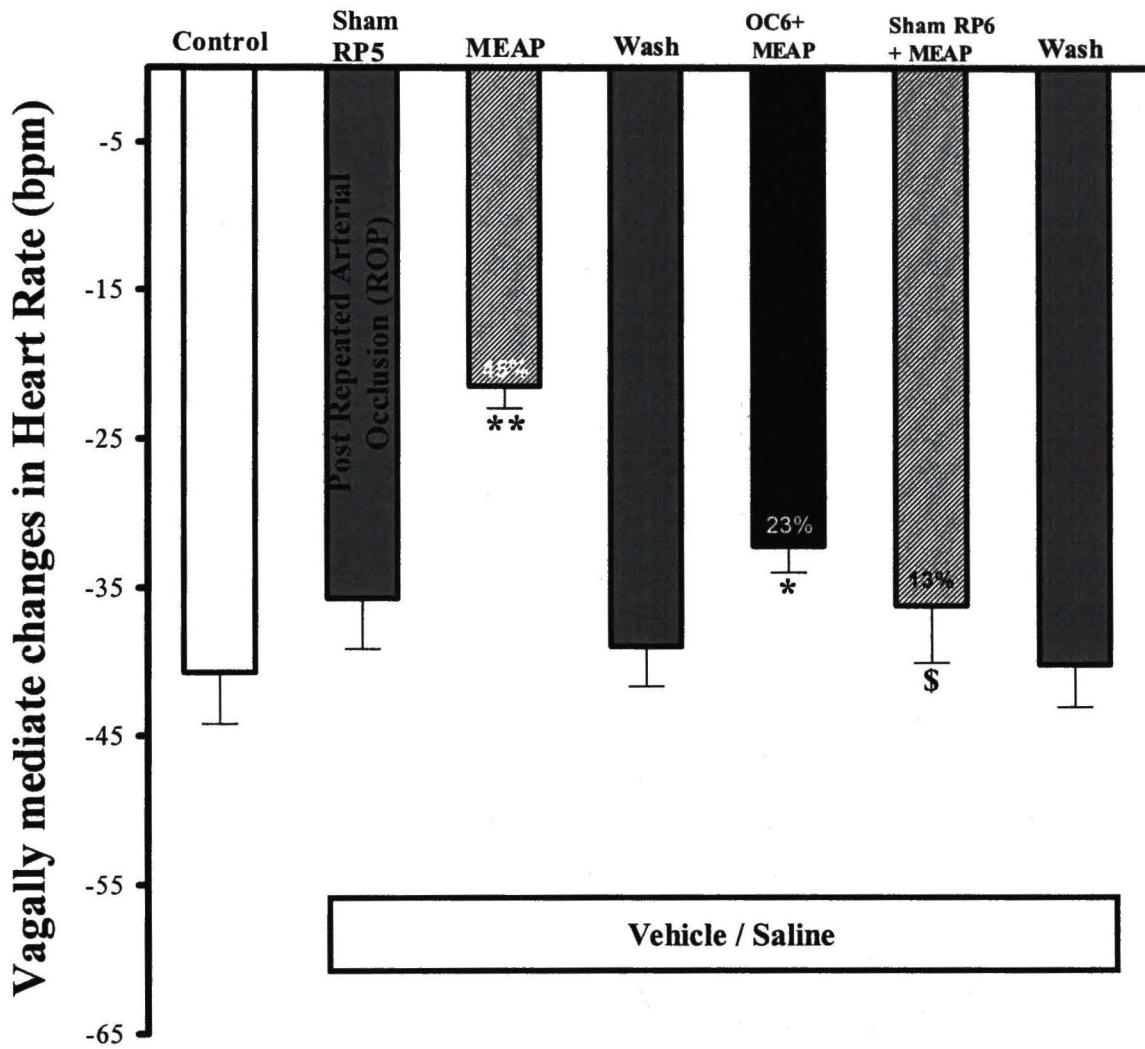


Figure 5(b)

IPC + BNTX

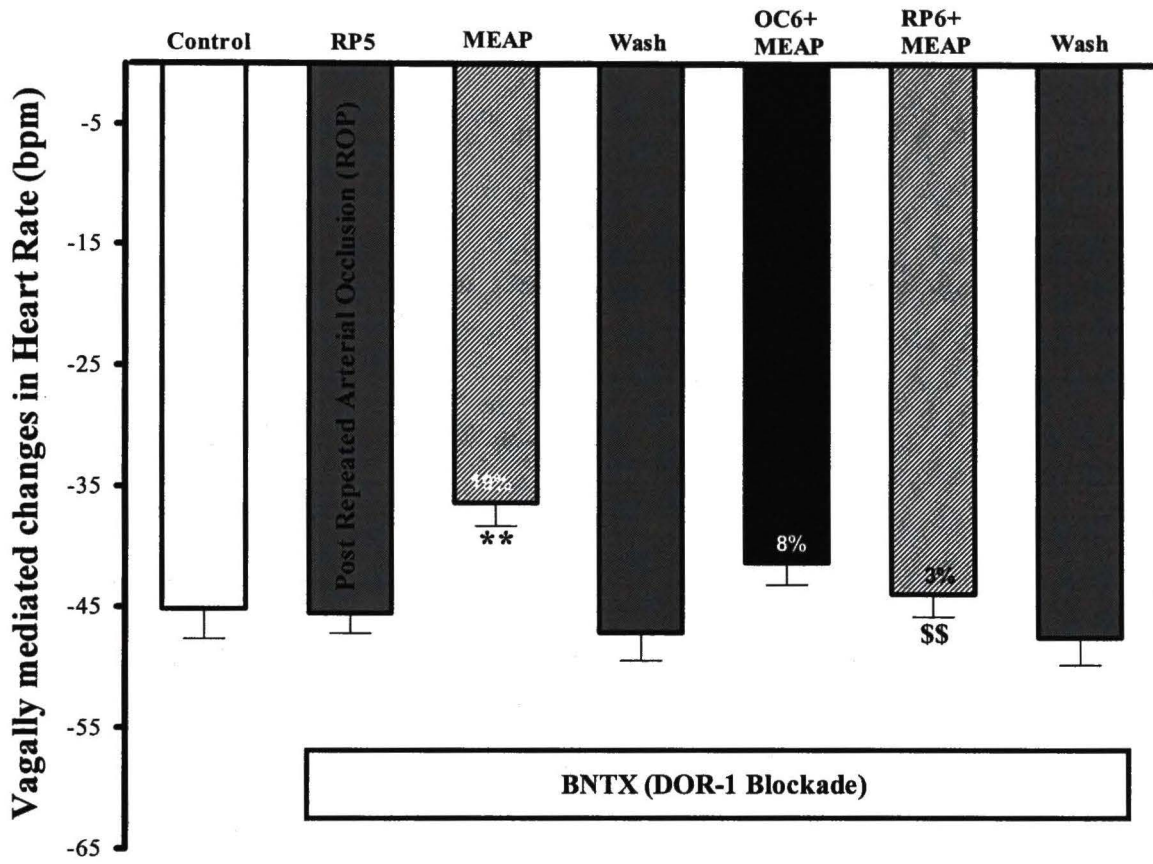


Figure 6

CHAPTER III

Cholinergic Location of Delta Opioid Receptors in Canine Atria and SA Node

Shekhar H. Deo, Matthew A. Barlow, Leticia Gonzalez, Darice Yoshishige, and James L. Caffrey

University of North Texas Health Science Center

Department of Integrative Physiology

3500 Camp Bowie Boulevard

Fort Worth, TX 76107

Corresponding author: James L. Caffrey

University of North Texas Health Science Center

Department of Integrative Physiology

3500 Camp Bowie Boulevard

Fort Worth, TX 76107

Tel. No. 817-735-2085

jcaffrey@hsc.unt.edu

Keywords: DOR, Opioids, Vagal function

ABSTRACT

Delta opioid receptors (DORs) are associated with ischemic preconditioning and vagal transmission in the SA node and atria. Although functional studies suggested DORs are prejunctional on parasympathetic nerve terminals, their precise location remains unconfirmed. DORs were co-localized in tissue slices and synaptosomes from the canine right atrium and SA node along with cholinergic and adrenergic markers, vesicular acetylcholine transporter (VACHT) and tyrosine hydroxylase (TH). Synapsin I immunofluorescence verified the neural character of tissue structures and isolated synaptosomes. Acetylcholine and norepinephrine measurements suggested the presence of both cholinergic and adrenergic synaptosomes. Fluorescent analysis of VACHT and TH signals indicated that more than 80% of the synapsin positive synaptosomes were of cholinergic origin and less than 8% were adrenergic. DORs co-localized 75-85% with synapsin in tissue slices from both atria and SA node. The co-localization was equally strong (85%) for nodal synaptosomes but less so for atrial synaptosomes (57%). Co-localization between DOR and VACHT was 75-85% regardless of the source. Overlap between DOR and TH was uniformly low ranging from 8-17%. Western blots with synaptosomal extracts confirmed two DOR positive bands at molecular weights corresponding to those reported for DOR monomers and dimers. The abundance of DOR was greater in nodal synaptosomes than in atrial synaptosomes; largely attributable to a greater abundance of monomers in the SA node. The abundant nodal and atrial DORs

predominantly associated with cholinergic nerve terminals supports the hypothesis that prejunctional DORs regulate vagal transmission locally within the heart.

INTRODUCTION

Enkephalins, the presumed endogenous agonists for the delta opioid receptor (DOR) are abundant in the heart (20, 26, 39). Although locally administered enkephalin produces robust physiological responses in heart (10-13, 33), the location of the DORs mediating these responses remains a matter of discussion (5, 21, 27). Myocardial enkephalin content is relatively low (20, 39), and the enzymes that degrade enkephalin are both aggressive and pervasive (19,36). Enkephalin mediated changes in cardiac function are difficult to demonstrate in the absence of nerve traffic (5, 18, 33). These observations suggest that cardiac enkephalins are primarily paracrine in character and the DORs mediating their effects do so by moderating local neurotransmission. When neurotransmitters were administered locally, the myocardial effects of enkephalin were eliminated suggesting that the opioid receptors mediating these responses were located prejunctionally on the nerve terminals innervating the heart (5, 10, 18, 33).

DORs belong to the super family of G-protein coupled, seven transmembrane receptors (34). The identification of the sequence of the receptor protein has made immunochemical quantification and localization of the DOR possible. Despite evidence for a single DOR amino acid sequence (16), physiological and biochemical studies support the existence of two functional subtypes of the DOR. Farias et al (13) demonstrated subtype specific bimodal actions for DORs in canine SA node. The DOR-1

phenotype improved the vagal transmission in the SA node while DOR-2 phenotype impaired it. The predicted net effect would then depend on the concentration of enkephalin locally and the relative proportion of receptors assuming each receptor phenotype.

A working hypothesis based on cultured cell systems suggests that DOR-1 phenotype couples to $G_{s\alpha}$ and DOR-2 to $G_{i\alpha}$ (8). DOR-1, $G_{s\alpha}$ coupling thus increases the adenylyl cyclase activity, intra-neuronal calcium and facilitates acetylcholine release to improve the vagal transmission. In contrast, DOR-2 coupling reduces cyclase activity and impairs vagal transmission. Excitatory $G_{s\alpha}$ -coupled receptors were also more efficient and were active at lower opioid doses (8). The local membrane environment appeared to determine which of the opposing receptor phenotypes predominated.

Cardiac DORs participate in the cardioprotection mediated by ischemic preconditioning (IPC) (31, 32). DOR stimulation also reduced arrhythmias and preserved the viability of isolated cells and organs (25, 35). The location of the responsible receptors remains undefined but studies *in vitro* (21, 27, 35, 39) support the widely held presumption that post-junctional DORs are involved. Intrinsic adrenergic cells, cardiomyocytes, adipocytes, fibroblasts and resident leucocytes are all potential sites for non-neural DORs (21, 27, 29, 35).

Opioids however, traditionally function as neuromodulators that moderate neurotransmitter release and considerable support for this view is evident in other parts of the nervous system (1, 14, 24, 25, 40). Acute functional responses in heart are consistent with the neural thesis and suggest a substantial proportion of myocardial DORs are located prejunctionally on parasympathetic nerves. However, a discrete location for DOR in heart remains unsettled. The present study combines immunofluorescent, cytochemical and biochemical methods to demonstrate that DORs concentrated in the canine SA node and atria are strongly associated with cholinergic nerve fibers and isolated synaptosomes and not with nearby adrenergic structures.

MATERIALS AND METHODS

Canine right atrial and sinus node tissues were obtained from mixed gender, adult (15-25 kg) mongrel dogs. The Institutional Animal Care and Use Committee in compliance with the National Institutes of Health Guide for the Care and Use of Laboratory Animals approved all procedures. Animals were anesthetized with pentobarbital sodium (32.5 mg/kg), intubated, and mechanically ventilated initially at 225 ml·min⁻¹·kg⁻¹ with room air. A right thoracotomy exposed the right heart between ribs three and four. The heart was briefly fibrillated with a surface electrode, the cardiac tissues were excised and either fixed in paraformaldehyde or frozen at -20°C.

SA node from the three dogs was fixed in 4% paraformaldehyde for 2 hours and progressively equilibrated in 15% and 30% sucrose solutions. The fixed nodal tissue was embedded in OCT-4583 (Sakura Fine Technical Co. Ltd.; Tokyo, Japan), and stored frozen at -90°C.

Preparation of Cardiac Synaptosomes: SA nodal and right atrial tissues were dissected free from fat and connective tissue. Tissues were minced in iced 0.32M sucrose and digested with collagenase in a shaking water bath for 60-90 min at 37°C. The collagenase (Worthington, 200 U/gram of wet weight) was prepared in a HEPES buffered salt solution (HBSS) containing mmol/L: HEPES 50 (pH 7.4), NaCl 144, KCl 5, CaCl₂ 1.2, MgCl₂ 1.2 and glucose 10 (38). Partially digested tissues were collected by low-speed

centrifugation (1000 x g) for 5 min at 4°C. The tissue pellet was suspended in four volumes of 0.32M sucrose solution and homogenized in a Teflon/glass homogenizer. The homogenate was centrifuged at 650 g for 10 min at 4°C and the supernatant was collected. The pellet was suspended again in four volumes of 0.32M sucrose, homogenized and centrifuged again at 650 g for 10 min at 4°C. The two supernatants were combined and the constituent synaptosomes were separated by centrifugation at 20,000g for 20 min at 4°C. The enriched synaptosome pellet was suspended in 500 µl/gm of HBSS per original wet tissue weight and purified further by discontinuous gradient centrifugation. The synaptosomal suspension was layered on 1.2 M sucrose and centrifuged at 20,000g for 120 min at 4°C. Purified synaptosomes were retrieved by pipette from the 0.32M/1.2M sucrose interface. The synaptosomes were either stored at -20°C or fixed by mixing with equal volumes of 4% paraformaldehyde.

Immunocytochemistry: Fixed synaptosomes obtained from SA node or right atrial sources were centrifugally dispersed using a cyto-centrifuge (CytoPro 7620; Wescor INC., Logan, UT) onto pre-charged glass slides at 1000 rpm. Each slide contained 60µl of synaptosomes (13-35 µg protein). Specific antisera for DOR (Rabbit anti-DOR), vesicular acetylcholine transporter (Goat anti-VACHT) (2) and tyrosine hydroxylase (Mouse anti-TH) (4) were obtained commercially from Chemicon Intl., Chicago, IL and Synapsin I (Goat anti-SYN) was obtained from Santa Cruz Biotechnology, Santa Cruz, CA. Synaptosomes were reacted with specific antibodies at the dilutions indicated in Table 1 for 12-18 hours at 4°C. After incubating with primary antibodies the sections

were rinsed in phosphate-buffered saline (PBS) and then incubated with the secondary antibodies (listed in Table 1) for 60 min in the dark. The slides were rinsed in PBS and sealed under cover slips with Fluormount G reagent (Electron Microscopy Sciences, Hatfield, PA). Slides were examined by fluorescent microscopy.

Immunohistochemistry: Fixed SA node tissues from three dogs were sectioned by cryostat (12 μ m, Vibratome UltraPro 5000; St. Louis, MO) perpendicular to the SA node artery and the slices were mounted on charged slides. The dilutions for the primary and secondary antibodies are listed in Table 2. Sections were examined using fluorescent microscopy at 10-40X magnification or confocal microscopy at 40X magnification.

Control: Control slides for synaptosomes as well as tissue sections were incubated with equal protein concentration of isotype specific immunoglobulin (IgG) matched with the IgG class of the respective primary antisera (Vector Laboratories Inc.; Burlingame, CA). In addition, the exposure time required to acquire images for the experimental slides under the fluorescent microscope was matched for the corresponding control slides.

Fluorescent Microscopy:

Specimens were examined with Olympus AX70 Fluorescence Imaging System with automatic photomicrography (Olympus America Inc., Center Valley, PA). Alexa Fluor 488 was imaged with the fluorescent filter using 482 nm excitation and 536 nm emission wavelengths, while Alexa Fluor 594 was imaged with the filter using 562 nm excitation

and 624 nm emission wavelengths. The images shown were acquired at the surface of the specimens in two dimensions.

Quantification of dual immunolabeling:

Synaptosomes:

The numbers of dual labeled e.g. DOR-VACHT and DOR-TH synaptosomes were analyzed and quantified with ImagePro Plus 5.1 software (Media Cybernetics, INC., 8484 Georgia Avenue, Silver Spring, MD 20910). All counts were performed in the fluorescent microscope using the 40X objective. Two mounted synaptosomes slides were prepared from each animal for each treatment (antibody pairing). Five microscopic fields were analyzed from each slide. The resulting ten analyses were averaged and treated statistically as one value. Co-localization of DOR with selected synaptosomal targets of interest (SYN, VACHT and TH) was calculated as a (yellow/red) percentage.

Nodal Tissue Sections:

The numbers for co-localization of DOR-VACHT and DOR-TH in neural varicosities were analyzed using Image J 1.35 software (Developed by Dr. Wayne Rasband at Research Services Branch, National Institute of Mental Health, Bethesda, Maryland, USA). In each tissue slice, co-localization was specifically quantified in the wall of the nodal artery, in the adjacent nodal tissue and among the nearby atrial muscle cells. The co-localization counts in each field were quantified digitally at 10X. Two adjacent sections from three different animals were analyzed for co-localization of DOR

and VAcHT, and DOR and TH. The DOR overlap with cholinergic and adrenergic structures was again expressed as a percentage.

Western Blot: Cardiac synaptosomes obtained as described above were analyzed for protein content (Lowry) and 20 μ g of each preparation were separated by SDS-PAGE, transferred to nitrocellulose membranes and probed with primary anti DOR and synapsin antibodies (1:1000 rabbit polyclonal antibodies, Chemicon Intl., Chicago, IL). The membranes were incubated with horseradish peroxidase (HRP) labeled anti-rabbit gamma globulin (1:10,000; Amersham Biosciences). The blots were developed with ECL kit (Super signal West Dura Extended Duration Substrate; Pierce Biotechnology; Rockford, IL). Densitometric analysis of the bands was performed using the image-analysis software (Scion; National Institutes of Health, Bethesda, MD). The relative band intensities were expressed as a DOR/SYN ratio as mean \pm SEM for the three individual experiments.

Estimation of Synaptosomal Acetylcholine: Synaptosomal acetylcholine content was estimated by fluorospectrometry with Amplex Red[®]. Synaptosomal acetylcholine was hydrolyzed with added acetylcholine esterase (Sigma-Aldrich; St. Louis, MO) and the choline was converted to betaine and hydrogen peroxide with choline oxidase (Sigma-Aldrich; St. Louis, MO). The peroxide was quantified by reaction with added HRP (Sigma-Aldrich; St. Louis, MO) and Amplex Red[®] (Invitrogen-Molecular Probes; Eugene, OR) to generate the highly fluorescent product resorufin. The final assay was

conducted in 50mM Tris, pH 8.0 with 10,000 U/ml acetylcholine esterase, 4 U/ml HRP, 0.4 U/ml choline oxidase and 1U/ml Amplex Red®. The fluorescence was recorded at excitation and emission wavelengths of 563nm and 587nm, respectively at 500 volts with AB2 software in an Aminco-Bowman Series 2 Luminescence Spectrometer (SLM-Aminco; Urbana, IL). Values were compared with choline standards.

Estimation of Synaptosomal Norepinephrine (NE):

Atrial and SA nodal synaptosomes (11-30 µg of protein) were extracted in 1N acetic acid and 0.02 N HCL, boiled and neutralized with 1.5 M Tris at pH 8.6. The catecholamines were extracted with alumina (Bioanalytical System Inc.; West Lafayette, Indiana), eluted with 0.1M perchloric acid (Fischer Scientific; Fair Lawn, NJ) and separated by HPLC on a reverse-phase C18 analytical column (150mm X 3.9mm, 5µm, Waters Corporation; Milford, Massachusetts). Norepinephrine was eluted with 5mM lithium acetate (Sigma-Aldrich; St. Louis, MO), 2.0 mM sodium 1-heptanesulfonate (Sigma-Aldrich; St. Louis, MO), 100 µM EDTA (Sigma-Aldrich; St. Louis, MO), and 40% methanol (Fischer Scientific; Fair Lawn, NJ). quantified coulometrically using of ESA Coulchem III detection system. DHBA (3, 4-Dihydroxydenzylamine) was used as the internal standard.

Statistical Methods:

All data are means and standard errors. Differences were evaluated with ANOVA and post hoc analysis was performed with Tukey's test for multiple cross comparison and

Dunnett's test for multiple comparisons to control. Differences determined to occur by chance with a probability <0.05 were deemed statistically significant.

RESULTS

1. Tissue Sections:

A. Nodal Arterial Sections:

i. Morphological description:

The SA node artery traverses the long axis of the SA node and serves as a reliable marker for orientation within the node. The junction of tunica media and tunica adventitia in the wall of the nodal artery is also a reliable location in which to demonstrate autonomic nerves. The arterial wall served as a representative site in which to probe the relationship between DORs and autonomic nerve terminals. Intense green fluorescent labeling for DOR concentrated on punctuate varicose processes within the wall of the nodal artery. These strings of beaded fluorescence appeared as predicted at the junction of tunica media and tunica adventitia encircling the arterial lumen. Co-localizing neural peptide targets (SYN, VACHT and TH) appeared as red filamentous profiles in the same area as that of the DOR.

The Figures 1A and 1B illustrate the same nodal arterial cross-section immunolabeled for DOR and synapsin (SYN), respectively. The merged image in Figure 1C illustrates significant areas of overlap between SYN and DOR particularly at the junction of tunica media and tunica adventitia. There were two other areas of concentration and co-localization, the endothelium and the presumed pacemaker area.

Figure 1D is an example of an identical control merged image of a serial section in which isotype specific immunoglobulin was substituted for the two primary antibodies. Figure 2A and 2B represent similar images for another section localizing DOR and the cholinergic marker VACHT in the same general regions of the section. The merged image 2C illustrates a significant degree of overlap of the DOR signal with VACHT presumably representing cholinergic varicosities. Figure 3A presents a higher magnification (40X) of the vessel wall in Figure 2C observed under confocal microscope. The image clearly demonstrates intense discrete areas of co-localization between DOR and VACHT in both the outer vessel wall and within the endothelium. Progressive confocal images confirmed the co-localization of the two labels in the same visual volumes. Figure 4 illustrates another representative section through the nodal artery immunostained in this case for DOR and the adrenergic marker tyrosine hydroxylase. The labeling for DOR and TH was similar to that describe above. Both labels were again concentrated in the outer vessel wall and in the endothelium. While there appears to be continued signal overlap within the endothelium, the merged image, Figure 4C, clearly suggests that the DOR and TH are labeling different structures within the outer wall. These tissue images suggest that DOR preferentially localizes with cholinergic fibers within the nodal artery wall and not with nearby adrenergic structures.

ii. Quantification:

DOR labeling in these autonomic nerve terminals was quantified with image analysis software and expressed as a relative fraction for each arterial cross-section.

Figure 5 illustrates percent co-localization for DOR relative to SYN, VACHT and TH in the nodal artery wall (Figure 5; black bars). About 75% of the synapsin positive nerve terminals in the arterial wall were DOR-positive. The majority of those DOR positive (85%) structures are also positive for the cholinergic marker, VACHT. In contrast, DOR localization with TH was near 8%. Thus, a significant proportion of DORs were associated with nerves in the arterial wall and the vast majority of those nerves were cholinergic rather than adrenergic in character. The antibody controls for these slides were consistently non-reactive when analyzed for the same structural areas and at the same time exposures.

B. Nodal Tissue:

i. Morphological Description:

The SA node is composed of loose connective tissue, pacemaker cells near the artery and atrial myocytes that are progressively better organized structurally as one moves from the node into the atria (23). The presumed pacemaker tissues are outside the vessel wall in the lower left quadrant of Figures 1-4. Though not illustrated in the images, DAPI stained nuclear profiles indicated the area was densely populated with non-contractile cells. DOR-positive and VACHT-positive structures in this quadrant distributed in similar percentages to that above among the synapsin positive nerves fibers. Once again, 80% of the nerves were DOR positive. The number of apparent co-localizations between DOR and TH were by comparison equally few in numbers at 10%.

ii. Quantification:

As illustrated in Figure 5, a DOR positive signal was consistently recorded from 80% of the synapsin positive nerve terminals. The DOR signal was also similarly co-localized 81% of the time with VACHT and only 10% of the time with TH. Once again, a large proportion of DOR are closely associated with cholinergic nerve terminals in the SA node and much less so if at all with adrenergic nerve terminals.

C. Right Atrial Muscle:

i. Morphological Description:

Figure 3B illustrates atrial muscle section at higher magnification (40X) not far from the SA node artery. The cells sectioned parallel to their long axes provide a clear illustration of a network of DOR positive nerve fibers enveloping the atrial myocytes. The DOR signals appeared to be organized as intermittent varicosities parallel to the surface of the myocytes. The tissue section was also stained for VACHT that co-localized with DOR 76% of the time. The image illustrates occasional intense VACHT positive, DOR negative cholinergic fibers mixed with the DOR-positive fibers. Staining for DOR and TH in among the atrial myocytes in serial sections from each of the same animals provided much lower rates of co-localization.

ii. Quantification:

Figure 5 illustrates numerically equal percentages for DOR/SYN and DOR/VACHT co-localizations of 76% in among the atrial myocytes. DOR/TH

localizations were recorded only 17% of the time. The somewhat larger co-localization of DOR with TH in areas populated by myocytes suggests potential differences between the degree of opioid influence over pacemaker and contractile activities.

2. Synaptosomes:

Morphological description:

Synaptosomes are spheres of nerve membranes that form following disruption of the terminal nerve fibers. Such spheres are generally devoid of nuclear material and thus do not stain with DAPI. However, synaptosomes do contain neurotransmitter vesicles and presumably during formation, may enclose other buoyant cell particulates and cytoplasmic constituents. Synaptosomes were prepared from SA node and right atrium and were immunolabeled for the target peptides, DOR, SYN, VACHT, and TH. When centrifugally dispersed on charged slides in appropriate concentrations, immunolabeled synaptosomes in the microscope field appear as fluorescent stars in a dark field. Fluorescent signals and their respective quantitative co-localizations were based on software analysis of the digital images.

Quantification:

SA node Synaptosomes:

Synapsin labeling verified the synaptosomal character of the dispersed particulate and served to normalize the relative numbers of DOR, VACHT, and TH positive synaptosomes. As illustrated on the right in Figure 6, 80% of the synaptosomes

were cholinergic and fewer than 10% were adrenergic. Even higher percentages (85%) of the synaptosomes had expressed DORs. In addition to the DOR/SYN co-localization profiles, limited numbers of DOR negative but SYN-positive and DOR-positive and SYN-negative were also evident on the synaptosomal slides. The SYN-positive but DOR-negative synaptosomes likely derive from adrenergic nerves and other non-autonomic nerves that do not bear axon terminal DORs.

A direct comparison between cholinergic and adrenergic synaptosomes regarding the distribution of DORs indicates that 82% of the cholinergic synaptosomes from the SA node express DOR while only 8% of adrenergic synaptosomes do so. DORs appear to be preferentially associated with cholinergic nerve terminals by a wide margin in the SA node. There were small percentages of synaptosomes observed outside of DOR-VACHT co-localization profiles. The VACHT-positive but DOR-negative profiles may represent a subset of DOR agonist-resistant cholinergic fibers. The VACHT-negative but DOR-positive profiles may be DORs derived from contaminating non-synaptosomal membranes derived from atrial myocytes, fibroblasts or adipocytes all of which reportedly express DOR. The 8% TH/DOR co-localization represents a low fractional distribution on an already much smaller number of TH/SYN positive adrenergic synaptosomes.

The control slides in which the isotype specific IgG was substituted for the primary target antibody of interest were uniformly unreactive with the secondary antibodies.

Right Atrial Synaptosomes:

The fractional ~10:1 distribution of VAcHT relative to TH-positive synaptosomes from atria was remarkably similar to the estimates described above for synaptosomes isolated from the SA node. Fractional estimates for DOR-positive profiles among the total atrial synaptosomes were significantly lower at 57%. Once more, expressed DORs were preferentially concentrated on VAcHT-positive, cholinergic synaptosomes compared with TH-positive, adrenergic synaptosomes at a now familiar ~8:1 ratio. As illustrated in Figure 6, anti-DOR antibodies immunolabeled 79% of the cholinergic synaptosomes and only 11% of the adrenergic synaptosomes. These results confirm the consistent preferential association of DOR with presumed, pre-junctional cholinergic nerve terminals.

Western Blot:

Western blots were conducted with synaptosomal proteins to provide additional support for the identity of synaptosomal DOR. The Figure 7A illustrates immunoreactive bands obtained with rabbit anti-DOR and rabbit anti-synapsin antibodies on nodal and atrial synaptosomes. Equal amount of proteins were loaded in each well. The image illustrates distribution of synaptosomal proteins in six lanes with the first three lanes for

synaptosomes from the SA node of three different dogs and the next three lanes for right atrial synaptosomes from the same animals. Two immunoreactive bands were evident for DOR corresponding to molecular weights of ~75 KDa and 50 KDa. The estimated molecular weights were consistent with those reported for monomers and dimers of the DOR in other species. Parallel gels were immunostained for synapsin I and an appropriate molecular weight band was quantified by densitometry at ~100 KDa. The density for each DOR band was normalized to the density for the total synapsin I in the same sample.

Figures 7B graphically presents the mean DOR/SYN ratios for both the SA node and the right atrial synaptosomes. The open bar illustrates the total DOR/SYN ratio for both tissues. The black and gray bars illustrate the ratios for the respective monomers and dimers. DOR abundance was significantly greater in SA node synaptosomes than in companion atrial synaptosomes. The difference was largely attributable to a greater abundance of monomers in the nodal synaptosomes. These immunoblot analyses corroborate that the immunoreactivity for the synaptosomal DOR is consistent with its reported molecular mass. Finally, DOR may be more concentrated in the SA node.

Table 3 illustrates the mixed neurotransmitter content of the synaptosome preparations. Acetylcholine content was greater in nodal synaptosomes as compared to the right atrium. The acetylcholine content was likewise much greater than that for NE in both SA node and right atrium, supporting the predominantly cholinergic character of the

synaptosomes as isolated from both SA node and right atrium. In addition, NE content in the nodal adrenergic synaptosomes was greater than the atrial synaptosomes.

DISCUSSION

The observations presented support the suggestion that a large proportion of DORs in heart are on postganglionic prejunctional parasympathetic nerve terminals. Both tissue sections and isolated synaptosomes were internally consistent with 80% of the immunolabeled DORs associated with VACHT labeled cholinergic membranes. More specifically 85% of the nodal synaptosomes were DOR-positive and 82% of cholinergic synaptosomes were DOR-positive. If these two populations are the same, then 100% of the DOR-positive nodal synaptosomes may be cholinergic. That estimate would represent an upper limit for DOR expression on nodal cholinergic synaptosomes. If the DOR/VACHT-positive synaptosomes were not all coincident, the minimum overlap predicted would approximate 68%. The DOR positive synaptosomes from atrial muscle were a smaller proportion (57%) of the total synaptosomes suggesting greater numbers of non-autonomic nerve terminals in the atria. The remaining 43% synapsin positive membranes were DOR-negative. Of the total synaptosomes, 8% were adrenergic. About 79% of the atrial synaptosomes were cholinergic and 79% of those were DOR-positive. Thus, the estimated upper limit of the total DOR positive synaptosomes in atria would be 62%. Since two estimates of total DOR positive synaptosomes were similar (57% and 62%), all of the atrial DORs may be associated with cholinergic nerve endings. The DOR/VACHT relationships were not evaluated in ventricular tissue and whether the same atrial pattern persists in the ventricle remains unclear.

The presence of DOR on the adrenergic synaptosomes was significantly lower for synaptosomes from both SA node and atrium. Few (6-8%) of the total synaptosomes were adrenergic and a small percentage of the adrenergic synaptosomes were DOR positive. Thus, less than 1% of the total synaptosomes were dual DOR/TH labeled. Although opioids can modify adrenergic function and norepinephrine secretion in the heart, the receptor is most likely kappa opioid in character (3, 18, 33). Whether the DOR/TH positive membranes are physiologically significant or represent a methodological background cannot be determined from the current data. Contamination of cholinergic synaptosomes during isolation with soluble TH, might contribute to false positive results of this small magnitude.

Intact cultured ventricular cardiomyocytes and resident adrenergic cells isolated from myocardial digests, both convincingly immunostain positive for DOR (21,27). Membranes from both of these cell types might contaminate the synaptosomal preparation. Resident adrenergic cells do not seem sufficiently abundant to account for the very high DOR/SYN staining. However, small numbers of chromaffin-like cells might easily account for the much lower DOR/TH co-localization. Contamination with DOR associated with the potentially far more abundant cardiomyocyte membranes is less easily ruled out but could again represent an atrial-ventricular or species difference in the origin of the cells. Cell surface DORs are commonly associated with lipid rafts and routinely exchange with intracellular DOR pools. The receptor exchange may involve caveolar membranes and DOR protein was reportedly isolated in rat caveolin rich

cardiomyocyte membrane fractions (25). The isolation of cardiac caveolar membranes and synaptosomes both involve similar density gradient centrifugation systems and some degree of cross contamination might be expected. The DOR observed in tissue slices was co-localized 80% of the time with nerves and DOR staining near myocytes appeared to be discretely associated with neural structures. Thus, the evidence for a neural association is significant. Despite the absence of convincing DOR/myocyte localizations, 20% of DOR positive staining was quantified morphometrically as SYN-negative and thus remained unaccounted. DORs actively traffic between the cell surface and substantive pools of intracellular receptor. The specific identification of DORs in cultured cardiomyocytes and cultured myocardial chromaffin cells suggests perhaps that those DORs were available on the surface of the cultured cells but may have been otherwise sequestered in intact tissues and thus unavailable to interact with labeling antibodies.

The high acetylcholine content relative to norepinephrine combined with the VAcHT and TH labeling supports the supposition that the synaptosomes isolated in the current study were predominantly cholinergic in character. The greater acetylcholine content in the nodal synaptosomes relative to atrial synaptosomes suggests that the cholinergic innervation of the node may be better equipped to make and release acetylcholine than its atrial counterpart.

Western blot analysis confirmed that the DOR immunoreactivity extracted from the synaptosomes was consistent with the expected molecular mass of the receptor based on reports from other animals (1, 16, 28). The proportionately greater density of the DOR bands from nodal synaptosomes relative to atrial synaptosomes was consistent with the parallel results from immunostaining of the synaptosomes and their quantification under the fluorescent microscope. The Western analysis also indicated that DOR monomers were proportionately greater in the nodal synaptosomes. Both electrophoresis and fluorescent microscopy suggested that nodal synaptosomes expressed approximately 50% more receptor than atrial synaptosomes. The Western analysis suggested that much of the difference resulted from greater numbers of DOR monomers in the SA node. Monomers and dimers could represent the functional DOR-1 and DOR-2 phenotypes of the receptor. The formation of DOR monomers also appears to precede their internalization and presumed inactivation (9). Although opioids regulate the vagal control of both heart rate and atrial contraction, it remains unclear whether the greater numbers of DORs or greater numbers of monomers in the SA node translates into difference in function or sensitivity.

Synapsin I is a membrane protein situated specifically on synaptic vesicles and nerve terminals. VACHT is a membrane-associated transporter that moves acetylcholine into the synaptic vesicles in cholinergic nerves (2). The close association of DORs, synapsin and VACHT strongly suggests that the majority of DORs in the atria and SA node are on postganglionic prejunctional parasympathetic nerve terminals.

The strong co-localization of DOR and VAcHT within fibers innervating of the nodal artery wall and endothelium was surprising. Images from the confocal microscope confirmed the discrete neural tract-like appearance of these signals suggesting that opioids may moderate coronary blood flow as well as heart rate and contractility.

The heart receives qualitatively different parasympathetic innervations from the dorsal motor nucleus of vagus and nucleus ambiguus (6, 7). The nucleus ambiguus projects faster type B fibers and the dorsal motor nucleus projects slower type C fibers. Two-third of the fibers to the right heart originate from the nucleus ambiguus and these faster fibers are likely responsible for the fast phasic regulation of heart rate and atrial contraction associated with vagal stimulation. Similar percentages of atrial cholinergic fibers are DOR positive and approximately two-thirds of the vagal response *in vivo* is routinely susceptible to blockade by administered enkephalin. These observations suggest the hypothesis that the DOR positive vagal fibers originate in the nucleus ambiguus and opioids moderate their acute vagal responses. Alternatively, the enkephalin resistant, DOR negative fibers would then be responsible for slower vegetative or background control of heart rhythms.

The low incidence of DOR/TH-positive nerve terminals suggests the probable absence of DOR on adrenergic nerve terminals consistent with the failure of DOR stimulation to alter sympathetically mediated tachycardia (3, 18, 33). The apparent low level DOR/TH co-localization may in fact represent the failure of the method to resolve

DOR signals from nearby cholinergic nerve terminal membranes that are near the adrenergic synaptosomes.

In conclusion, the present study supports the hypotheses that DORs are located on the postganglionic prejunctional parasympathetic nerve terminals and the expression of DOR is significantly greater on the cholinergic nerve terminals than on the adrenergic nerve terminals in SA node and right atrium.

ACKNOWLEDGMENTS

The authors acknowledge the expert advice and assistance of Harlan Jones (Microbiology and Immunology) with the quantitative immunofluorescent analysis, Vidhya R. Rao (Pharmacology and Neuroscience) with the Western blot analysis, Robert Wordinger (Anatomy and Cell Biology) with the immunofluorescence and Ignacy Gryczynski (Center for Commercialization of Fluorescence Technology) with the confocal analysis. This study was supported in part by the American Heart Association Texas Affiliate.

REFERENCES

1. **Arvidsson U, Dado RJ, Riedl M, Lee JH, Law PY, Loh HH, Elde R and Wessendorf MW.** delta-Opioid receptor immunoreactivity: distribution in brainstem and spinal cord, and relationship to biogenic amines and enkephalin. *J.Neurosci.* 15: 2: 1215-1235, 1995.
2. **Arvidsson U, Riedl M, Elde R and Meister B.** Vesicular acetylcholine transporter (VACHT) protein: a novel and unique marker for cholinergic neurons in the central and peripheral nervous systems. *J.Comp.Neurol.* 378: 4: 454-467, 1997.
3. **Barlow MA, Deo S, Johnson S and Caffrey JL.** Vagotonic effects of enkephalin are not mediated by sympatholytic mechanisms. *Exp.Biol.Med.(Maywood)* 231: 4: 387-395, 2006.
4. **Baryla J, Greniuk G and Lakomy M.** The adrenergic and cholinergic innervation of the thyroid chicken gland. *Folia.Morphol.(Warsz)* 62: 3: 247-249, 2003.
5. **Caffrey JL, Mateo Z, Napier LD, Gaugl JF and Barron BA.** Intrinsic cardiac enkephalins inhibit vagal bradycardia in the dog. *Am.J.Physiol.* 268: 2 Pt 2: H848-55, 1995.

6. **Cheng Z and Powley TL.** Nucleus ambiguus projections to cardiac ganglia of rat atria: an anterograde tracing study. *J.Comp.Neurol.* 424: 4: 588-606, 2000.
7. **Cheng Z, Powley TL, Schwaber JS and Doyle FJ.** Projections of the dorsal motor nucleus of the vagus to cardiac ganglia of rat atria: an anterograde tracing study. *J.Comp.Neurol.* 410: 2: 320-341, 1999.
8. **Crain SM and Shen KF.** After chronic opioid exposure sensory neurons become supersensitive to the excitatory effects of opioid agonists and antagonists as occurs after acute elevation of GM1 ganglioside. *Brain Res.* 575: 1: 13-24, 1992.
9. **Farias M, Jackson K, Johnson M and Caffrey JL.** Cardiac enkephalins attenuate vagal bradycardia: interactions with NOS-1-cGMP systems in canine sinoatrial node. *Am.J.Physiol.Heart Circ.Physiol.* 285: 5: H2001-12, 2003.
10. **Farias M, Jackson KE, Yoshishige D and Caffrey JL.** Cardiac enkephalins interrupt vagal bradycardia via delta 2-opioid receptors in sinoatrial node. *Am.J.Physiol.Heart Circ.Physiol.* 284: 5: H1693-701, 2003.
11. **Farias M, Jackson K, Stanfill A and Caffrey JL.** Local opiate receptors in the sinoatrial node moderate vagal bradycardia. *Auton.Neurosci.* 87: 1: 9-15, 2001.
12. **Farias M, Jackson K, Yoshishige D and Caffrey JL.** Bimodal delta-opioid receptors regulate vagal bradycardia in canine sinoatrial node. *Am.J.Physiol.Heart Circ.Physiol.* 285: 3: H1332-9, 2003.

13. **Fields HL, Emson PC, Leigh BK, Gilbert RF and Iversen LL.** Multiple opiate receptor sites on primary afferent fibres. *Nature* 284: 5754: 351-353, 1980.
14. **Fryer RM, Pratt PF, Hsu AK and Gross GJ.** Differential activation of extracellular signal regulated kinase isoforms in preconditioning and opioid-induced cardioprotection. *J.Pharmacol.Exp.Ther.* 296: 2: 642-649, 2001.
15. **Gaveriaux-Ruff C, Peluso J, Befort K, Simonin F, Zilliox C and Kieffer BL.** Detection of opioid receptor mRNA by RT-PCR reveals alternative splicing for the delta- and kappa-opioid receptors. *Brain Res.Mol.Brain Res.* 48: 2: 298-304, 1997.
16. **Gross GJ.** Role of opioids in acute and delayed preconditioning. *J.Mol.Cell.Cardiol.* 35: 7: 709-718, 2003.
17. **Gu H, Barron BA, Gaugl JF and Caffrey JL.** Dynorphin, naloxone, and overflow of norepinephrine during cardiac nerve stimulation in dogs. *Am.J.Physiol.* 263: 1 Pt 2: H153-61, 1992.
18. **Howells RD, Kilpatrick DL, Bailey LC, Noe M and Udenfriend S.** Proenkephalin mRNA in rat heart. *Proc.Natl.Acad.Sci.U.S.A.* 83: 6: 1960-1963, 1986.
19. **Huang MH, Wang HQ, Roeske WR, Birnbaum Y, Wu Y, Yang NP, Lin Y, Ye Y, McAdoo DJ, Hughes MG, Lick SD, Boor PJ, Lui CY and Uretsky BF.** Mediating delta-opioid-initiated heart protection via the beta2-adrenergic receptor: role of the intrinsic cardiac adrenergic cell. *Am.J.Physiol.Heart Circ.Physiol.* 293: 1: H376-84, 2007.

20. **Jackson KE, Farias M, Stanfill AS and Caffrey JL.** Transient arterial occlusion raises enkephalin in the canine sinoatrial node and improves vagal bradycardia.

Auton.Neurosci. 94: 1-2: 84-92, 2001.

21. **James TN.** Structure and function of the sinus node, AV node and his bundle of the human heart: part II--function. *Prog.Cardiovasc.Dis.* 45: 4: 327-360, 2003.

22. **Lewis RV.** Enkephalin biosynthesis in the adrenal medulla.

Adv.Biochem.Psychopharmacol. 33: 167-174, 1982.

23. **Lonergan T, Goodchild AK, Christie MJ and Pilowsky PM.** Presynaptic delta opioid receptors differentially modulate rhythm and pattern generation in the ventral respiratory group of the rat. *Neuroscience* 121: 4: 959-973, 2003.

24. **Paradis P, Dumont M, Belichard P, Rouleau JL, Lemaire S and Brakier-Gingras L.** Increased preproenkephalin A gene expression in the rat heart after induction of a myocardial infarction. *Biochem.Cell Biol.* 70: 7: 593-598, 1992.

25. **Patel HH, Head BP, Petersen HN, Niesman IR, Huang D, Gross GJ, Insel PA and Roth DM.** Protection of adult rat cardiac myocytes from ischemic cell death: role of caveolar microdomains and delta-opioid receptors. *Am.J.Physiol.Heart Circ.Physiol.* 291: 1: H344-50, 2006.

26. **Portoghese PS.** From models to molecules: opioid receptor dimers, bivalent ligands, and selective opioid receptor probes. *J.Med.Chem.* 44: 14: 2259-2269, 2001.

27. **Rabgaoui N, Slaoui-Hasnaoui A and Torreilles J.** Boomerang effect between [Met]-enkephalin derivatives and human polymorphonuclear leukocytes. *Free Radic.Biol.Med.* 14: 5: 519-529, 1993.
28. **Rousseau SJ, Jones IW, Pullar IA and Wonnacott S.** Presynaptic alpha7 and non-alpha7 nicotinic acetylcholine receptors modulate [3H]d-aspartate release from rat frontal cortex in vitro. *Neuropharmacology* 49: 1: 59-72, 2005.
29. **Schultz JE, Hsu AK and Gross GJ.** Ischemic preconditioning in the intact rat heart is mediated by delta1- but not mu- or kappa-opioid receptors. *Circulation* 97: 13: 1282-1289, 1998.
30. **Schultz JJ, Hsu AK and Gross GJ.** Ischemic preconditioning and morphine-induced cardioprotection involve the delta (delta)-opioid receptor in the intact rat heart. *J.Mol.Cell.Cardiol.* 29: 8: 2187-2195, 1997.
31. **Stanfill AA, Jackson K, Farias M, Barlow M, Deo S, Johnson S and Caffrey JL.** Leucine-enkephalin interrupts sympathetically mediated tachycardia prejunctionally in the canine sinoatrial node. *Exp.Biol.Med.(Maywood)* 228: 8: 898-906, 2003.
32. **Surratt CK and Adams WR.** G protein-coupled receptor structural motifs: relevance to the opioid receptors. *Curr.Top.Med.Chem.* 5: 3: 315-324, 2005.
33. **Takasaki Y, Wolff RA, Chien GL and van Winkle DM.** Met5-enkephalin protects isolated adult rabbit cardiomyocytes via delta-opioid receptors. *Am.J.Physiol.* 277: 6 Pt 2: H2442-50, 1999.

34. **Urbani A, Bongiorno L, Marini M, Zona C and Roda LG.** Hydrolysis of leucine enkephalin and its association to the K562(S) erythroleukaemic cell line. *Immunopharmacology* 27: 2: 119-130, 1994.
35. **Varga EV, Li X, Stropova D, Zalewska T, Landsman RS, Knapp RJ, Malatynska E, Kawai K, Mizusura A, Nagase H, Calderon SN, Rice K, Hruby VJ, Roeske WR and Yamamura HI.** The third extracellular loop of the human delta-opioid receptor determines the selectivity of delta-opioid agonists. *Mol.Pharmacol.* 50: 6: 1619-1624, 1996.
36. **Whittaker VP, Michaelson IA and Kirkland RJ.** The separation of synaptic vesicles from nerve-ending particles ('synaptosomes'). *Biochem.J.* 90: 2: 293-303, 1964.
37. **Younes A, Pepe S, Barron BA, Spurgeon HA, Lakatta EG and Caffrey JL.** Cardiac synthesis, processing, and coronary release of enkephalin-related peptides. *Am.J.Physiol.Heart Circ.Physiol.* 279: 4: H1989-98, 2000.
38. **Zhang X, Bao L, Arvidsson U, Elde R and Hokfelt T.** Localization and regulation of the delta-opioid receptor in dorsal root ganglia and spinal cord of the rat and monkey: evidence for association with the membrane of large dense-core vesicles. *Neuroscience* 82: 4: 1225-1242, 1998.

LEGENDS

Figure 1: Fluorescent images illustrate DOR (green, Figure 1A) and synapsin positive (red, Figure 1B) nerve terminals at the junction of tunica media and tunica adventitia in the wall of the SA nodal artery. The merged image (Figure 1C) superimposes the fluorescence to illustrate areas of co-localization. Figure 1D is identical control merged image of a serial section in which isotype-specific immunoglobulin was substituted for primary antibodies. The fluorescent images were acquired at 10X magnification in a standard fluorescent microscope. White scale bars in the lower right of each image indicate 50 μ m. Labels: tunica media (TM), tunica adventitia (TA), endothelium (ET), pacemaker region (PM), atrial muscle (M).

Figure 2: Fluorescent images illustrate DOR (green, Figure 2A) and VACHT positive (red, Figure 2B) nerve terminals at the junction of tunica media and tunica adventitia in the wall of the SA nodal artery and in the adjacent nodal parenchyma (lower left quadrant). The merged image (Figure 2C) superimposes the fluorescence to illustrate areas of co-localization. The fluorescent images were acquired at 10X magnification in a standard fluorescent microscope. White scale bars in the lower right of each image indicate 50 μ m. Labels: tunica media (TM), tunica adventitia (TA), endothelium (ET), pacemaker region (PM), atrial muscle (M).

Figure 3A illustrates a higher magnification (40X, scale bar = 10 μm) confocal image of part of the same vessel wall shown in 2C above. The image illustrates dense areas of DOR-positive cholinergic nerve terminals. Image 3B illustrates a nearby section of right atrial muscle that demonstrates co-localization of DOR-positive nerve fibers with cholinergic varicosities running parallel to the long axis of the atrial muscle fibers. The merged two-dimensional image was acquired at 40X and the scale bar = 10 μm . Labels: tunica media (TM), tunica adventitia (TA), endothelium (ET), atrial muscle (M), cholinergic nerves (CN).

Figure 4: Fluorescent images illustrate DOR (green, Figure 4A) and TH positive (red, Figure 4B) labeling near the SA nodal artery and in the adjacent nodal parenchyma. The majority of the TH labeling near the periphery of Figure 4B is autofluorescence illustrated to demonstrate the absence of TH labeling in the arterial wall. The merged image (Figure 4C) superimposes the fluorescence and reinforces the absence of TH co-localization with DOR positive nerve tracts within the vessel wall. The fluorescent images were acquired at 10X magnification in a standard fluorescent microscope. White scale bars in the lower right of each image indicate 50 μm . Labels: tunica media (TM), tunica adventitia (TA), endothelium (ET), atrial muscle (M).

Figure 5: Quantification in Tissue Sections: Estimation of proportions of DORs on nodal artery, nodal tissue and right atrial muscle based on co-localization percentages. The graph is the quantitative representation between DOR-positive areas in total (SYN),

cholinergic (VACHT) and adrenergic (TH) nerve terminals. The values illustrated are the DOR% in the respective nerve terminal. Note significantly higher percentage of DOR on cholinergic nerve terminals in arterial wall, nodal tissue and atrial muscle than on corresponding adrenergic structures. Values are means and standard error of the mean for three subjects. The symbol (**) indicate the number of co-localization in the cholinergic nerves were significantly different from that of adrenergic nerves $P < 0.01$.

Figure 6: Quantification in Synaptosomes: Estimation of proportions of DORs on SA nodal and right atrial synaptosomes based on co-localization percentages. The graph is the quantitative representation of DOR-positive synaptosomes from total (SYN), cholinergic (VACHT) and adrenergic (TH) nerve terminals. In addition, the figure also illustrates the percentages of cholinergic (VACHT/SYN) and adrenergic (TH/SYN) synaptosomes. The values illustrated are the DOR% in the respective nerve terminal in the first 3 groups of bars. The fourth and the fifth groups represent percentages of cholinergic and adrenergic synaptosomes. Note significantly higher percentage of DOR on cholinergic nerve terminals in nodal as well as atrial synaptosomes. Values are means and standard error of the mean for three subjects. The symbol (**) indicate the number of co-localization in the cholinergic nerves were significantly different from that of adrenergic nerves $P < 0.01$.

Figure 7: Verification of the presence of DOR on synaptosomes by western blot analysis. Image A demonstrates western blots with rabbit anti-DOR and rabbit anti-synapsin

antibodies. Proteins were derived from synaptosomes obtained from canine SA node and right atrium (n = 3). Lanes 1 to 3 represent proteins from SA node of dogs 1, 2 and 3, while lanes 4 to 6 represent proteins from right atrium of dogs 1, 2 and 3. Thus, lanes 1 and 4 represent nodal and atrial synaptosomal proteins, respectively from dog 1. Protein loading was 20µg/lane. As illustrated (Figure 7A), two immunoreactive bands were obtained for DOR at 75 KDa and 50 KDa. Figure 7B illustrates the densitometric analysis for the Western blots in Figure 7A. DOR intensities were normalized to synapsin (SYN) from the same extract. The white bars illustrate the total DOR/SYN intensity ratio and the black and the grey bars indicate similar ratios for monomers and dimers respectively. The graph illustrates significantly higher DOR protein content in SA node than in right atrium. Values are means and standard error of the mean for three subjects. The symbol (**) indicate the expression of total and monomeric DOR in SA node was significantly different from that in right atrium $P < 0.01$.

Table 1: Immunocytochemical Labeling of Synaptosomes

Targets	Primary Antibody Dilutions	Secondary Antibody Dilutions
SYN + DOR	Goat Anti-SYN (1:500) Rabbit Anti-DOR (1:500)	Donkey Anti-Goat Alexa Fluor 594 (1:500) Donkey Anti-Rabbit Alexa Fluor 488 (1:1000)
VACHT + DOR	Goat Anti-VACHT (1:5000) Rabbit Anti-DOR (1:500)	Donkey Anti-Goat Alexa Fluor 594 (1:500) Donkey Anti-Rabbit Alexa Fluor 488 (1:1000)
TH + DOR	Mouse Anti-TH (1:7500) Rabbit Anti-DOR (1:500)	Donkey Anti-Mouse Alexa Fluor 594 (1:500) Donkey Anti-Rabbit Alexa Fluor 488 (1:1000)

Table 2: Immunohistochemical Labeling for nodal tissue sections.

Targets	Primary Antibody Dilutions	Secondary Antibody Dilutions
SYN +	Goat Anti-SYN (1:1000)	Donkey Anti-Goat Alexa Fluor 594 (1:2000)
DOR	Rabbit Anti-DOR (1:250)	Donkey Anti-Rabbit Alexa Fluor 488 (1:1000)
VACHT +	Goat Anti-VACHT (1:10000)	Donkey Anti-Goat Alexa Fluor 594 (1:2000)
DOR	Rabbit Anti-DOR (1:250)	Donkey Anti-Rabbit Alexa Fluor 488 (1:1000)
TH +	Mouse Anti-TH (1:15000)	Donkey Anti-Mouse Alexa Fluor 594 (1:2000)
DOR	Rabbit Anti-DOR (1:250)	Donkey Anti-Rabbit Alexa Fluor 488 (1:1000)

Table 3: Values are means and standard error of means of acetylcholine and NE contents from SA nodal and right atrial synaptosomes (n=3)

	Acetylcholine (pmol/μg synaptosomal protein)	NE (fmol/μg synaptosomal protein)
SA Node	364.27 \pm 64.92	15.58 \pm 1.46
Right Atrium	72.35 \pm 30.54	5.13 \pm 0.54

Fig 1A
DOR
Nodal Artery

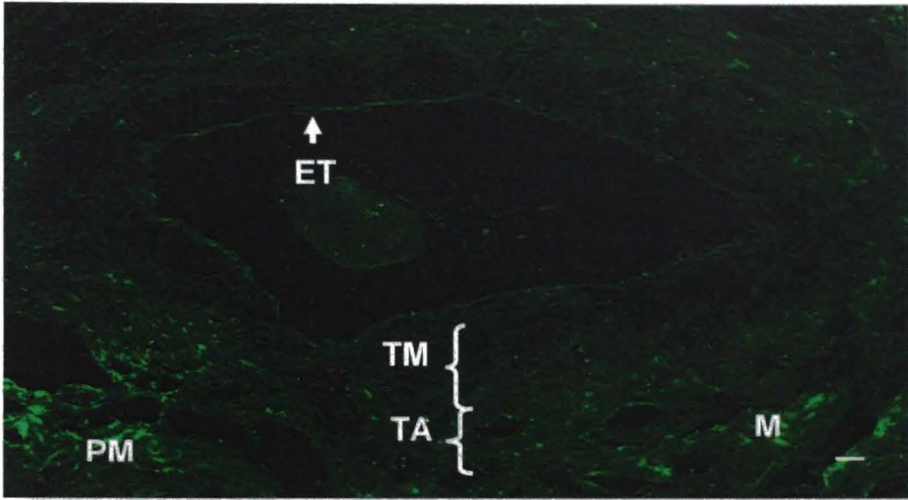


Fig 1B
Synapsin
Nodal Artery

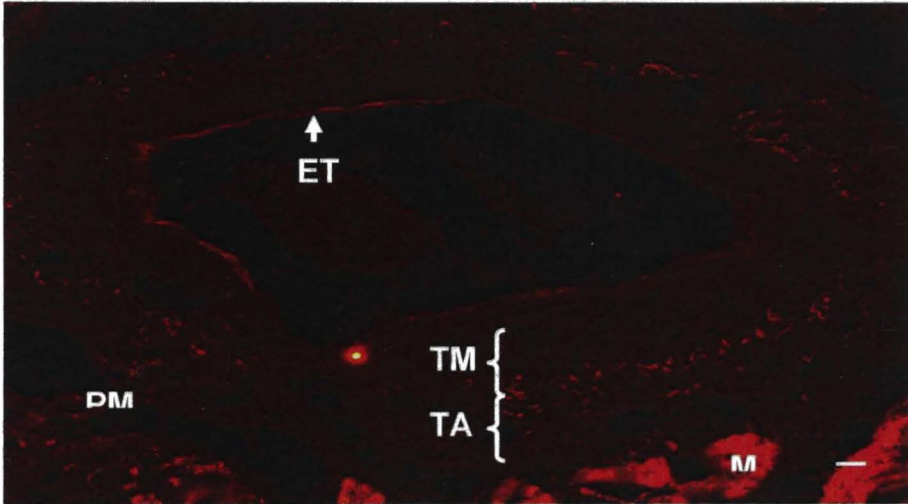


Fig 1C
Merged

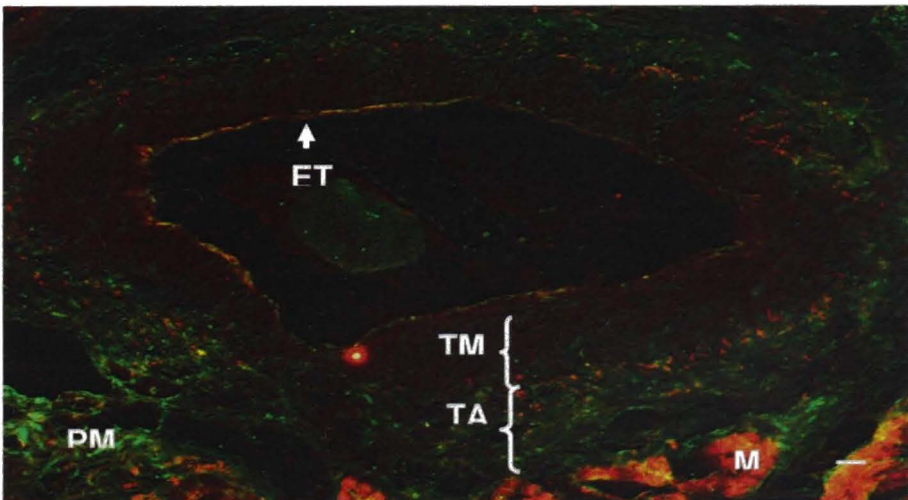


Fig 1D
Merged
Blank

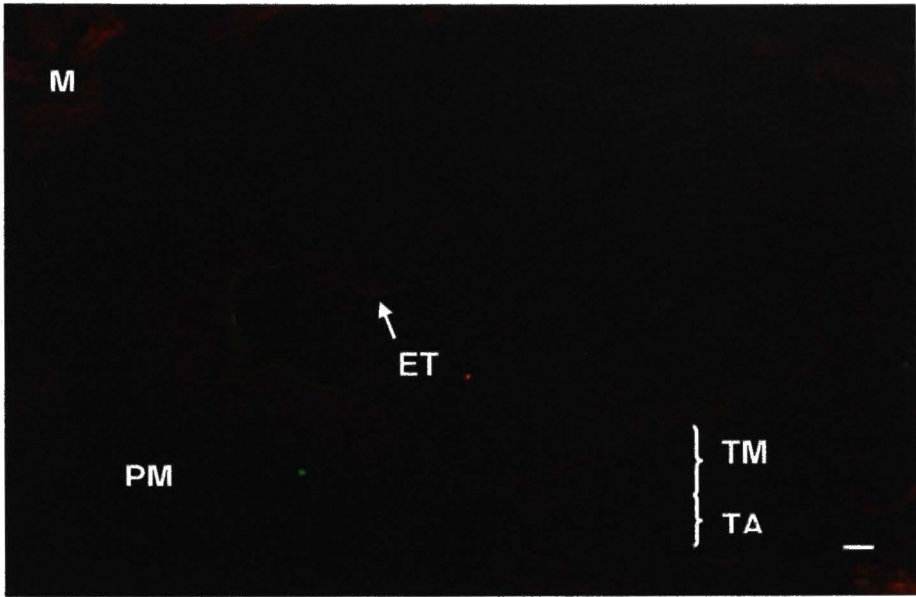


Fig.2A
DOR
SA Node

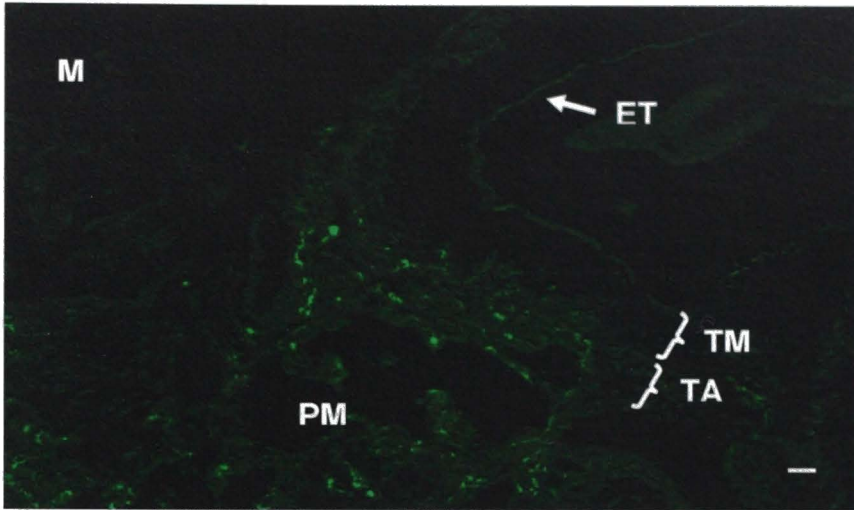


Fig.2B
VACHT
SA Node

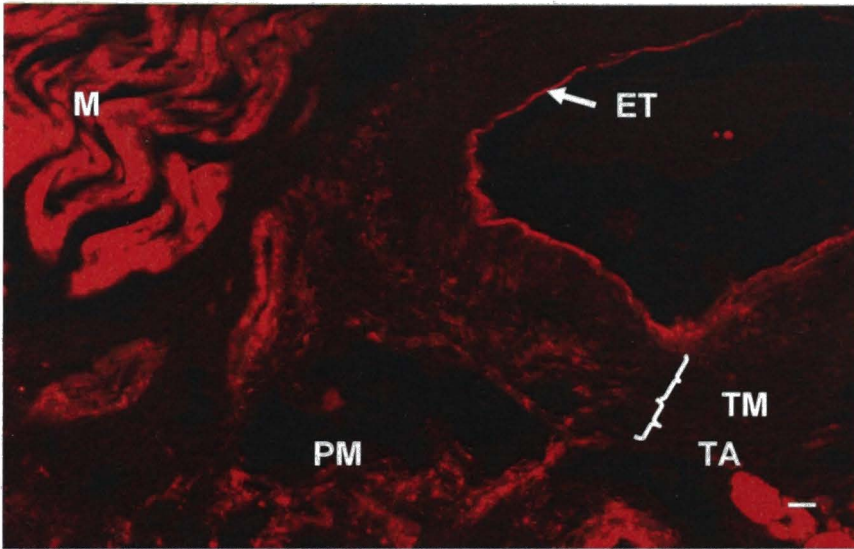


Fig.2C
Merged

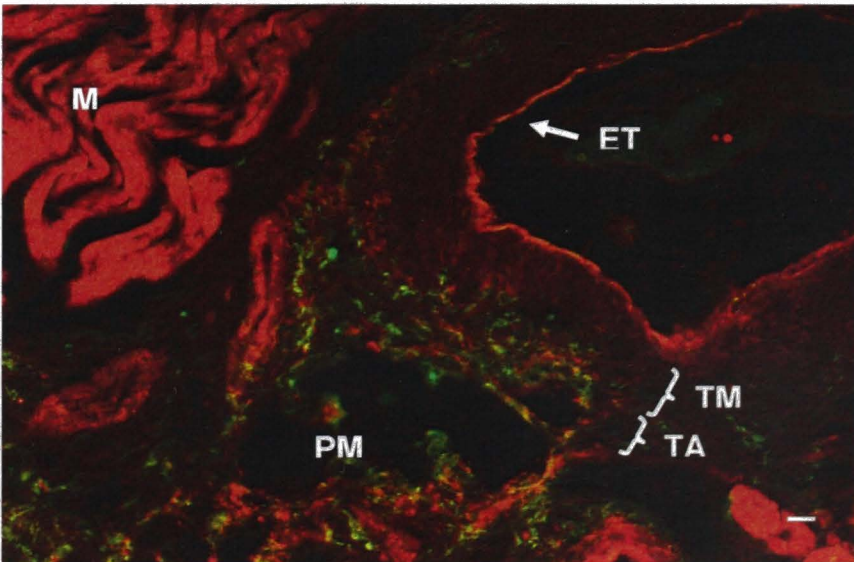


Fig. 3A
DOR/VACHT
Nodal Artery
Confocal 40X

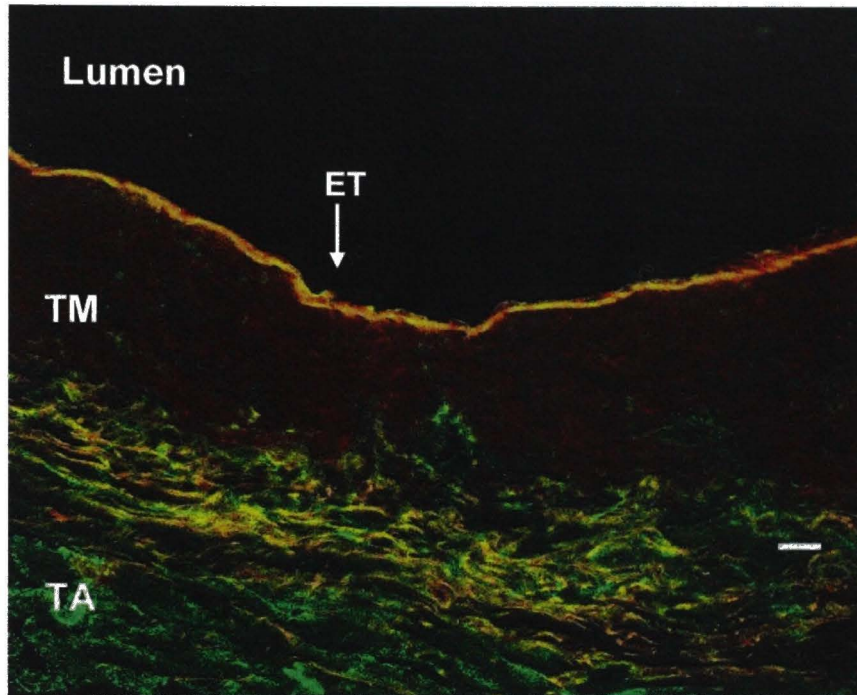


Fig. 3B DOR/VACHT
Atrial Myocytes 40X

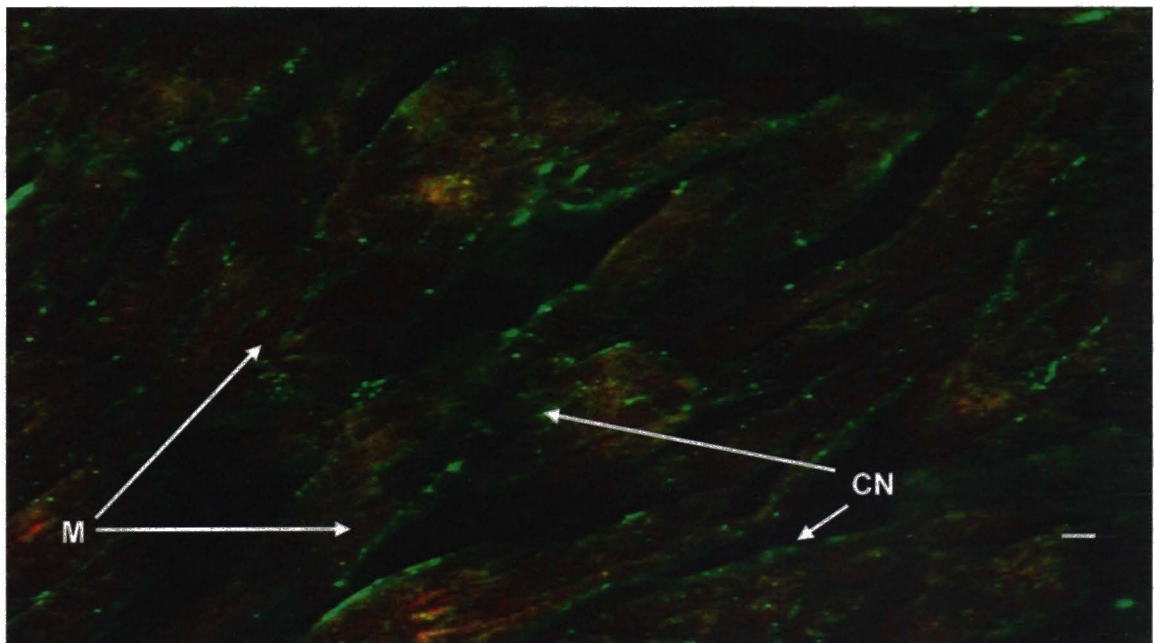


Fig. 4A
DOR
Nodal Artery

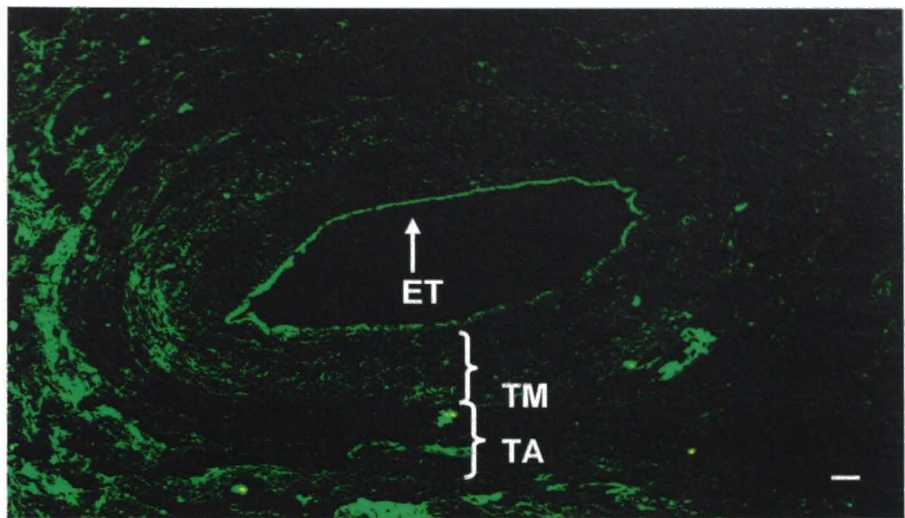


Fig. 4B
TH
Nodal Artery

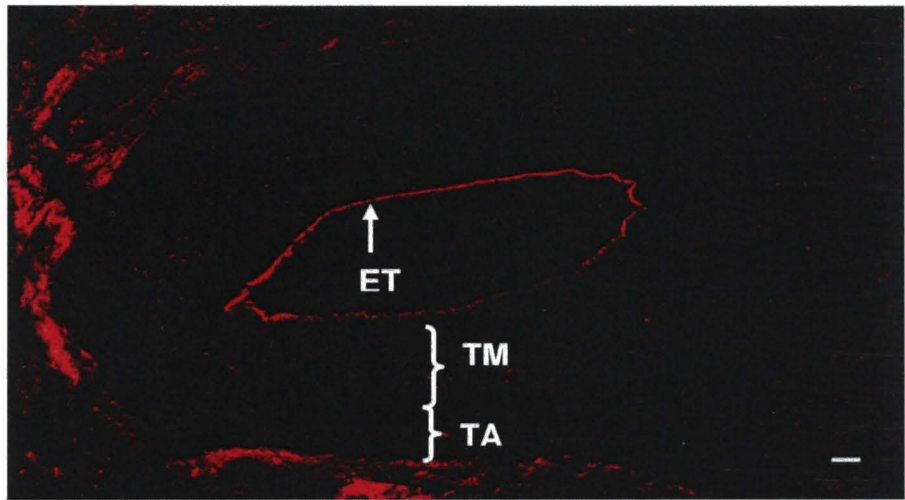


Fig. 4C
Merged

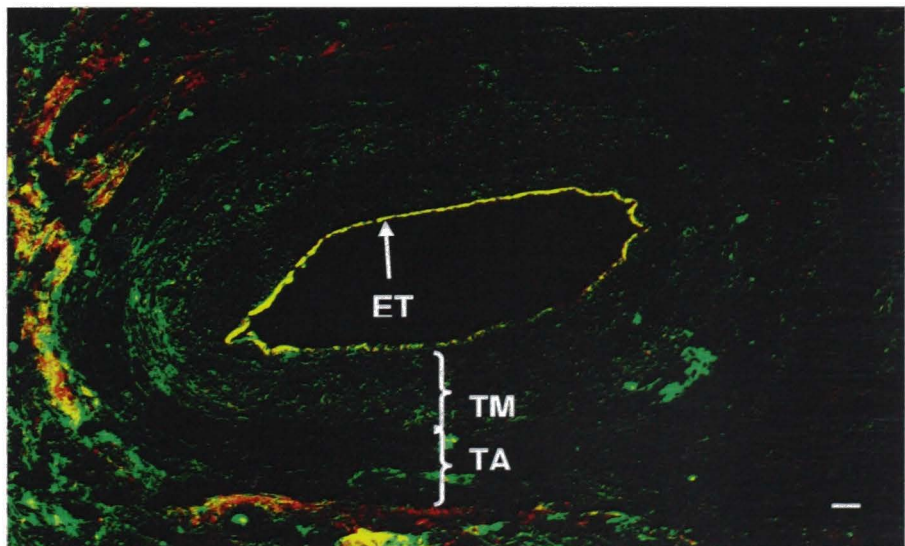


Figure 5

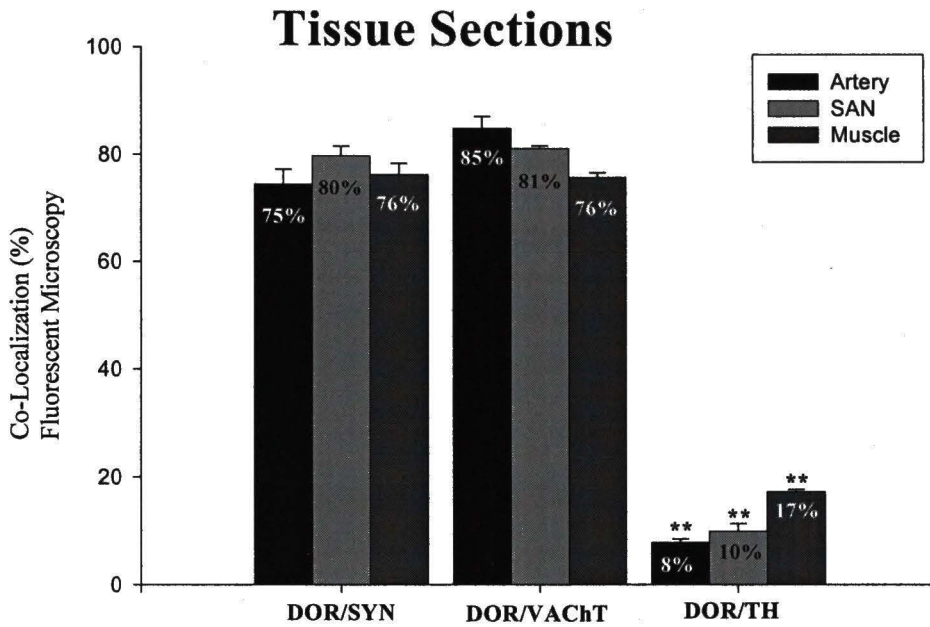


Figure 6

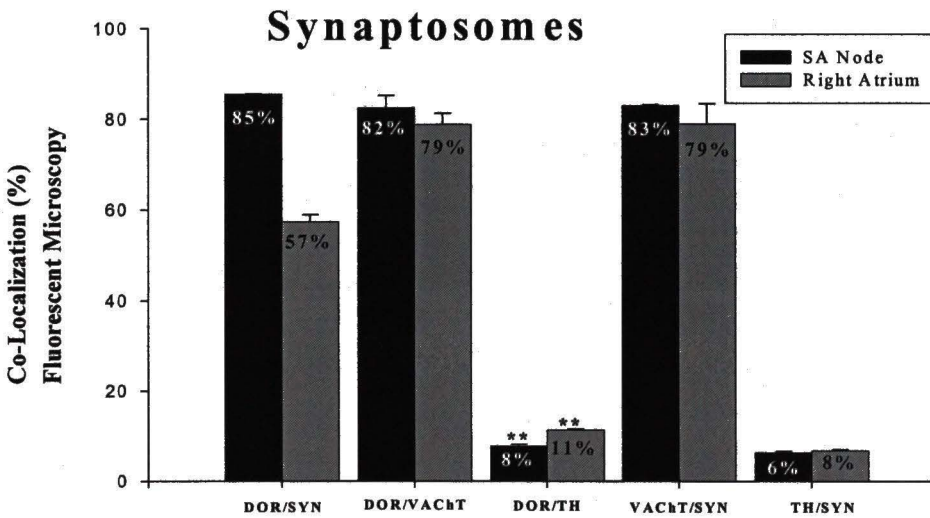
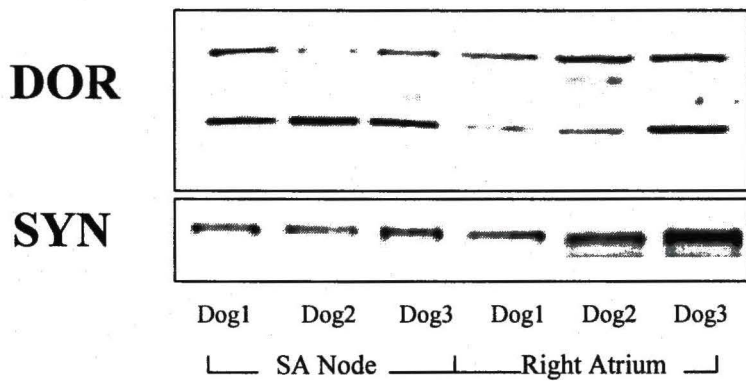
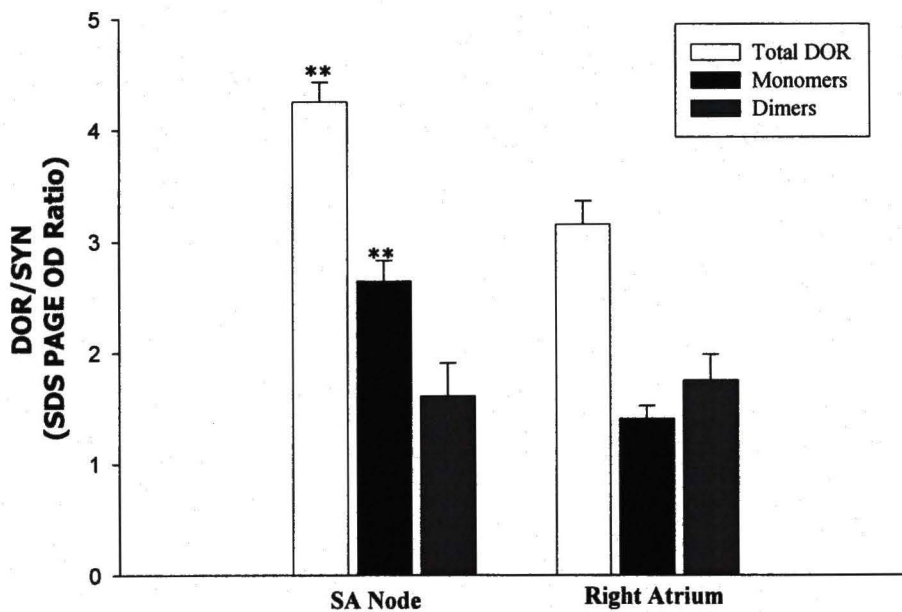


Figure 7
A



B

Synaptosomes Immunoblots



CHAPTER IV

SUMMARY AND CONCLUSIONS

- Preconditioning is required for the observed improvement of the vagal transmission.
- The vagotonic effect observed after preconditioning is mediated via DOR-1.
- The loss of DOR-2 vagolytic response was not restored by DOR-1 blockade, thus this loss is not mediated via DOR-1. The erosion of DOR-2 response was likely the result of its down regulation due to an interaction between preconditioning induced alterations in the nerve membrane environment and DOR-2 stimulation.
- Majority of the DORs are located on the post-ganglionic prejunctional parasympathetic nerve terminals and not on adrenergic nerve terminals in the canine SA node.

CHAPTER V

FUTURE STUDIES

The following studies are proposed to further clarify the role of DORs and their changing phenotypes in canine SA node.

1. To measure the proportion of DOR on the prejunctional parasympathetic nerve terminals following the preconditioning protocol using immunocytochemistry and western blot and correlate these changes with function *in vivo*.
2. Using cardiac synaptosomes, determine the association between DOR and GM1 using immunocytochemistry, western blot and co-immunoprecipitation techniques.
3. To determine the role of DOR phenotypes in health and disease.

